



Complex Permittivity of Polyaniline–Carbon Nanotube and Nanofibre Composites in the X-band

PMMA Composites

Darren A. Makeiff

Trisha Huber

Paul Saville

Defence R&D Canada – Atlantic

Technical Memorandum

DRDC Atlantic TM 2004-124

May 2005

Report Documentation Page				Form Approved OMB No. 0704-0188	
Public reporting burden for the collection of information is estimated to average 1 hour per response, including the time for reviewing instructions, searching existing data sources, gathering and maintaining the data needed, and completing and reviewing the collection of information. Send comments regarding this burden estimate or any other aspect of this collection of information, including suggestions for reducing this burden, to Washington Headquarters Services, Directorate for Information Operations and Reports, 1215 Jefferson Davis Highway, Suite 1204, Arlington VA 22202-4302. Respondents should be aware that notwithstanding any other provision of law, no person shall be subject to a penalty for failing to comply with a collection of information if it does not display a currently valid OMB control number.					
1. REPORT DATE 16 MAR 2005		2. REPORT TYPE		3. DATES COVERED -	
4. TITLE AND SUBTITLE Complex Permittivity of Polyaniline-Carbon Nanotube and Nanofibre Composites in the X-band. PMMA Composites				5a. CONTRACT NUMBER	
				5b. GRANT NUMBER	
				5c. PROGRAM ELEMENT NUMBER	
6. AUTHOR(S)				5d. PROJECT NUMBER	
				5e. TASK NUMBER	
				5f. WORK UNIT NUMBER	
7. PERFORMING ORGANIZATION NAME(S) AND ADDRESS(ES) Defence R&D Canada -Atlantic,PO Box 1012,Dartmouth, NS,CA,B2Y 3Z7				8. PERFORMING ORGANIZATION REPORT NUMBER	
9. SPONSORING/MONITORING AGENCY NAME(S) AND ADDRESS(ES)				10. SPONSOR/MONITOR'S ACRONYM(S)	
				11. SPONSOR/MONITOR'S REPORT NUMBER(S)	
12. DISTRIBUTION/AVAILABILITY STATEMENT Approved for public release; distribution unlimited					
13. SUPPLEMENTARY NOTES The original document contains color images.					
14. ABSTRACT see report					
15. SUBJECT TERMS					
16. SECURITY CLASSIFICATION OF:			17. LIMITATION OF ABSTRACT	18. NUMBER OF PAGES 58	19a. NAME OF RESPONSIBLE PERSON
a. REPORT unclassified	b. ABSTRACT unclassified	c. THIS PAGE unclassified			

This page intentionally left blank.

Complex Permittivity of Polyaniline–Carbon Nanotube and Nanofibre Composites in the X-band

PMMA Composites

Darren A. Makeiff

Trisha Huber

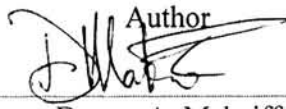
Paul Saville

Defence R&D Canada – Atlantic

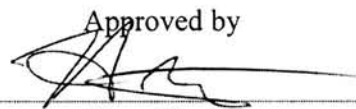
Technical Memorandum

DRDC Atlantic TM 2004-124

May 2005

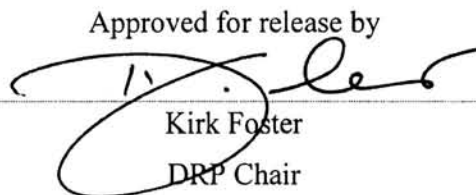
Author


Darren A. Makeiff

Approved by


Terry Foster

Head Dockyard Laboratory Pacific

Approved for release by


Kirk Foster

DRP Chair

Terms of release: The information contained herein is proprietary to Her Majesty and is provided to the recipient on the understanding that it will be used for information and evaluation purposes only. Any commercial use including use for manufacture is prohibited. Release to third parties of this publication or information contained herein is prohibited without the prior written consent of Defence R&D Canada.

Abstract

Polymer composites incorporating polyaniline (PAni) and multiwalled carbon nanotubes (MWNTs) as conductive filler were synthesized and characterized using FT-IR spectroscopy, SEM, TEM, and dc conductivity measurements. The pure nanocomposite powders were significantly more conductive than PAni, MWNT, or CNFs alone. PAni, MWNT, CNFs, PAni-coated MWNT (PAni-MWNT), and PAni-coated CNF (PAni-CNF) nanocomposites were also incorporated as conductive filler into the insulating matrix, PMMA, to produce a rigid and conductive composite material with well-defined shape. The microwave properties of these composites were examined by determining the complex permittivity from transmission-reflection waveguide measurements in the X-band (8-12 GHz). PMMA composites containing PAni-MWNT or PAni-CNFs poorer, while PMMA composites containing PAni and MWNT mixed *ex situ*ⁱ were better microwave absorbers than composites containing only PAni or MWNTs.

Résumé

Des composites polymères contenant de la polyaniline (PAni) et des nanotubes de carbone multiparois (NTMP) servant d'agents conducteurs ont été synthétisés et caractérisés par spectroscopie FTIR, MEB, MET et en mesurant la conductivité en courant continu. Les poudres de nanocomposites purs étaient substantiellement plus conductrices que la polyaniline, les NTMP ou les nanofibres de carbone (NFC) seuls. Des nanocomposites de polyaniline, de NTMP, de NFC, de NTMP recouverts de polyaniline (PAni-NTMP) et de NFC recouvertes de polyaniline (PAni-NFC) ont également été incorporés comme agents conducteurs dans la matrice isolante de PMMA pour produire un matériau composite rigide et conducteur ayant une forme bien définie. Les propriétés hyperfréquence de ces composites ont été examinées en déterminant la permittivité complexe à partir de mesures de transmission et de réflexion à l'aide d'un guide d'ondes dans la bande X (8-12 GHz). Les composites de PMMA contenant des PAni-NTMP ou des PAni-NFC se sont révélés être de moins bons absorbeurs de micro-ondes que les composites contenant de la polyaniline ou des NTMP seulement, alors que les composites de PMMA contenant de la polyaniline et des NTMP mélangés *ex situ*ⁱ se sont révélés être de meilleurs absorbeurs de micro-ondes.

ⁱ *In situ* is Latin meaning "inside the natural position or place." In the context of this report, *in situ* means in the (polymerization) reaction. In contrast, *ex situ* is Latin for "outside the natural position or place", which in this report means outside of the (polymerization) reaction, or post-polymerization.

This page intentionally left blank.

Cette page est intentionnellement laissée en blanc.

Executive summary

Introduction

This report summarizes preliminary studies on the investigation of the combination of conducting polymers (CPs) and carbon nanotubes (CNTs) as potential RAM. Organic CPs are excellent candidates for RAM because they are intrinsically strong microwave and mm-wave absorbers due to high conductivity at these frequencies. Furthermore, CPs alone or in composites are known to display broad-band microwave absorption absent in more traditional metal or carbon-fibre based materials. CNTs are also good candidates for RAM because they have high intrinsic conductivity and demonstrate favorable electromagnetic interference (EMI) shielding properties related to RAM. Typically, conductive networks in a radar absorbing material (RAM) enable incident electromagnetic (EM) radiation to be dissipated as heat, due to induced current flow within the material. Nanocomposites formed between CPs like polyaniline (PAni) and CNTs have demonstrated improved electrical properties over their individual constituents alone. Based on this premise, we were interested to see if PAni–CNTs incorporated into a polymer composite would lead to a similar improvement in microwave absorption relative to PAni or CNTs alone. In this report, PAni–CNT and PAni–CNF nanocomposites are synthesized using CNTs and CNFs purchased commercially. The preparation of composites containing PAni and CNTs or CNFs as conductive filler is also detailed in this report. These materials were characterized by FT-IR spectroscopy, SEM, TEM, conductivity, and complex permittivity in X-band (8-12 GHz).

Results

This report is divided into two parts: (1) the *in situ* synthesis and characterization of PAni–CNTs and CNFs nanocomposites, and (2) preparation and determination of the complex permittivity of PMMA composites containing (a) PAni, (b) CNTs, (c) CNFs, (d) PAni and CNTs, and (e) PAni and CNFs. PAni–CNTs and CNF nanocomposites were successfully synthesized *in situ* by the polymerization of aniline in the presence of CNTs or CNFs, respectively. PAni–CNT and CNF powders were more conductive than PAni, CNT, or CNFs alone, due to a PAni coating. When processed at a relatively low wt % in a PMMA matrix, the resulting composites had poorer microwave properties relative to similar composites with PAni, CNTs, or CNTs alone. In contrast, PMMA composites containing *ex situ* mixed PAni and CNTs displayed enhanced microwave properties. This was not the case when PAni and CNFs were mixed *ex situ*.

Significance

In order to fabricate an effective broad-band microwave absorber for RAM, such as a Jaumann layer device, the physical properties of potential materials must be examined in detail. These parameters may then be used to model the optimum structures for a multi-layer RAM device. This report provides preliminary evidence that composites incorporating both PAni and CNTs (i.e., MWNTs) exhibit interesting microwave properties, which can be controlled by varying the wt % of total PAni and CNTs, the ratio of PAni : CNTs, and the method of mixing PAni and CNTs. The fabrication of composite materials with tunable conductivity and absorption at microwave frequencies are important for modeling the

optimum structures of RAM, such as in a Jaumann layer device, and their subsequent fabrication.

The magnitude of microwave absorption is also dependent on the batch of PANi (i.e. synthetic conditions) and type of dopant used. Improvements need to be made with dispersing *in situ* PANi-CNTs (or CNFs) in a composite and nailing down the synthetic conditions to reliably produce PANi with the best microwave properties.

Future plans

Continuing work on this project may include:

Further optimization of synthesis parameters for various doped PANis to produce powders with optimum microwave properties. This would require further characterization for structure-activity correlations. Further improvements could also be made in the PANi-CNT synthesis, to control the uniformity and thickness of the PANi coating. It would also be advantageous to produce PANi-CNT nanocomposite powders that can be dispersed at the primary particle level. CNTs from a variety of commercial sources should be investigated as well.

The PMMA composites synthesized for this report should be characterized in greater detail. Further inspection of the microscopic structure and morphology of the presented composites may reveal details distinguishing good microwave absorbers from poor ones.

Other matrices besides PMMA for composites should be investigated as well. PANi-CNTs may be more compatible with other potential matrix polymers. These may include polystyrenes, polyvinylchlorides, polyvinylalcohols, epoxies etc.

This report only details the measurement of a few microwave properties over a narrow frequency range. Frequencies outside of the X-band should also be explored as well as other microwave properties such as transmission, absorption, reflection, EMI shielding effectiveness, and radar cross section should be investigated. However, different frequency ranges require different instrumentation.

Makeiff, D. A.; Huber, T.; Saville, P.. 2004. Complex Permittivity of Polyaniline/Carbon Nanotube and Nanofibre Nanocomposites in the X-band. DRDC Atlantic TM 2004-124, Defence R&D Canada – Atlantic.

Sommaire

Introduction

Le présent rapport résume des études préliminaires sur la possibilité de combiner des polymères conducteurs (PC) et des nanotubes de carbone (NTC) pour obtenir des matériaux absorbant les ondes radar (MAR). Les PC organiques sont d'excellents candidats pour élaborer des MAR parce qu'ils sont intrinsèquement d'excellents absorbeurs de micro-ondes et d'ondes millimétriques en raison de leur grande conductivité à ces fréquences. De plus, les PC seuls ou dans des composites absorbent les micro-ondes dans une large bande de fréquences, ce qui n'est pas le cas des matériaux plus courants à base de métaux ou de fibres de carbone. Les NTC sont également de bons candidats pour élaborer des MAR à cause de leur grande conductivité intrinsèque et de leurs bonnes propriétés de blindage contre les interférences électromagnétiques. Généralement, des réseaux conducteurs dans un matériau absorbant les ondes radar permettent de dissiper en chaleur le rayonnement électromagnétique incident à cause du courant induit dans le matériau. Les nanocomposites formés de PC comme la polyaniline (PAni) et les NTC ont de meilleures propriétés électriques que leurs constituants distincts. Sur la base de cette prémisse, nous avons cherché à déterminer si des PAni-NTC incorporés à un composite polymère apporteraient une amélioration comparable dans l'absorption des micro-ondes par rapport à la polyaniline seule ou aux NTC seuls. Le présent rapport traite de la synthèse de nanocomposites PAni-NTC et PAni-NFC, à partir de NTC et de NFC commerciaux. La fabrication des composites contenant de la polyaniline et des NTC ou des NFC comme agents conducteurs est également décrite en détail dans le rapport. Ces matériaux ont été caractérisés par spectroscopie FTIR, MEB, MET, et en mesurant la conductivité et la permittivité complexe dans la bande X (8-12 GHz).

Résultats

Ce rapport est divisé en deux parties : 1) la synthèse *in situ* et la caractérisation des nanocomposites PAni-NTC et PAni-NFC, et 2) la fabrication et la détermination de la permittivité complexe de composites de PMMA contenant a) de la polyaniline, b) des NTC, c) des NFC, d) de la polyaniline et des NTC, et e) de la polyaniline et des NFC. Des nanocomposites PAni-NTC et PAni-NFC ont été synthétisés avec succès *in situ* par la polymérisation de l'aniline en présence de NTC ou de NFC, respectivement. Les poudres de PAni-NTC et de PAni-NFC avaient une plus grande conductivité que la polyaniline, les NTC ou les NFC seuls à cause du revêtement de polyaniline. Quand ils étaient fabriqués avec un pourcentage en poids relativement faible dans une matrice de PMMA, les composites résultants avaient des propriétés hyperfréquence moins bonnes que des composites semblables n'utilisant seulement que de la polyaniline, des NTC ou des NFC. À l'opposé, les composites de PMMA contenant de la polyaniline et des NTC mélangés *ex situ* avaient de meilleures propriétés hyperfréquence, ce qui n'était pas le cas quand la polyaniline et les NFC étaient mélangés *ex situ*.

Importance des résultats

Il faut examiner en détail les propriétés physiques des matériaux candidats en vue de fabriquer un absorbeur de micro-ondes à large bande efficace pour les MAR, comme un dispositif à couche de Jaumann. Ces paramètres peuvent ensuite être utilisés dans la modélisation des structures optimales pour un dispositif à MAR multicouche. Ce rapport fait état de premières indications que les composites contenant à la fois de la polyaniline et des NTC (c.-à-d. les NTMP) ont des propriétés hyperfréquence intéressantes que l'on peut réguler en modifiant le pourcentage en poids de la quantité totale de polyaniline et de NTC, le rapport des quantités de polyaniline et de NTC, et la méthode de mélange de la polyaniline et des NTC. La fabrication de matériaux composites ayant une conductivité et une absorptivité hyperfréquence que l'on peut choisir à volonté est importante dans la modélisation des structures optimales pour les MAR, comme dans les dispositifs à couche de Jaumann, et pour leur fabrication par la suite.

L'importance de l'absorption des micro-ondes dépend également du lot de la polyaniline (c.-à-d. des conditions de synthèse) et du type de dopant utilisé. Il faudra apporter des améliorations à la dispersion *in situ* des PANi-NTC (ou NFC) dans un composite et établir clairement les conditions de synthèse pour fabriquer avec fiabilité de la polyaniline ayant les meilleures propriétés hyperfréquence.

Travaux futurs

La poursuite de ce projet pourrait inclure les travaux suivants :

Une optimisation plus poussée des paramètres de synthèse pour diverses polyanilines dopées afin de fabriquer des poudres ayant des propriétés hyperfréquence optimales. Cela exigerait une caractérisation plus poussée des relations structure-activité. D'autres améliorations pourraient également être apportées à la synthèse des PANi-NTC afin de réguler l'uniformité et l'épaisseur de la couche de polyaniline. Il serait également avantageux de fabriquer des poudres de nanocomposites PANi-NTC qui peuvent être dispersées au niveau des particules primaires. Il faudrait également examiner les NTC provenant de diverses sources commerciales.

Les composites de PMMA qui ont été synthétisés dans le cadre des travaux faisant l'objet du rapport devraient être caractérisés plus en détail. Un examen plus approfondi de la structure microscopique et de la morphologie des composites présentés pourrait révéler des particularités permettant de distinguer les bons et les médiocres absorbeurs de micro-ondes.

D'autres matrices que le PMMA devraient également être examinées pour les composites. Les PANi-NTC pourraient être plus compatibles avec d'autres matrices polymères, lesquelles pourraient inclure des polystyrènes, des composés de poly(chlorure de vinyle) et de poly(alcool de vinyle), des résines époxydes, etc.

Le présent rapport ne traite que de la mesure de quelques propriétés hyperfréquence sur une gamme de fréquences étroite. Les fréquences à l'extérieur de la bande X devraient également être étudiées, de même que d'autres propriétés hyperfréquence comme la transmission,

l'absorption, la réflexion, l'efficacité de blindage contre les interférences électromagnétiques et la section efficace radar. Toutefois, l'étude des différentes gammes de fréquences exige l'utilisation d'appareils de mesure distincts.

Makeiff, D.A.; Huber, T.; Saville, P.. 2004. Permittivité complexe de nanocomposites de polyaniline et de nanotubes et de nanofibres de carbone dans la bande X : composites de PMMA. RDDC Atlantique TM 2004-124. Defence R&D Canada – Atlantic.

Table of contents

Abstract.....	i
Executive summary	iii
Sommaire.....	v
Table of contents	viii
List of figures	x
1. Introduction	1
1.1 Microwave Properties.....	1
1.2 Polyaniline.....	2
1.3 Carbon Nanotubes	3
1.4 Polyaniline–Carbon Nanotube Nanocomposites.....	4
2. Experimental.....	5
2.1 Synthesis.....	5
2.1.1 Polyaniline.....	5
2.1.2 Polyaniline–Multiwalled Nanotube/Polyaniline–Carbon Nanofibre Nanocomposites	5
2.2 Poly(methyl methacrylate) Composites.....	6
2.3 Fourier Transform-Infrared Spectroscopy	6
2.4 Electron Microscopy	6
2.5 Conductivity Measurements.....	6
2.6 Permittivity Measurements.....	7
3. Results and Discussion	8
3.1 Synthesis.....	8
3.2 Microscopy	8
3.3 Fourier Transform-Infrared Spectroscopy	11
3.4 The DC Conductivity of Bulk Polyaniline–Carbon Nanofibre Nanocomposites	13
3.5 The DC Conductivity of Polyaniline–Multiwalled (Carbon) Nanotube Nanocomposites	16

3.6	Poly(methyl methacrylate) Composites.....	18
3.7	Conclusions	27
4.	References	30
	Distribution list.....	38

List of figures

Figure 1. Repeating structures of various forms of Polyaniline.	3
Figure 2. SEM images of a) uncoated CNFs, b) nanocomposite N1i, c) uncoated MWNTs, and d) nanocomposite N2i.....	9
Figure 3. TEM images of a) uncoated CNFs, b) nanocomposite N1i, c) uncoated MWNTs, d) and nanocomposite N2i.....	10
Figure 4. Possible Polyaniline–carbon nanostructure complex structures (carbon nanostructures (CNS)= carbon nanotubes or carbon nanofibres).....	11
Figure 5. FT-IR spectra (KBr) of a) PAni–pTsA, b) N1i (8 wt % MWNT), c) N1i (19 wt % MWNT), d) N1i (27 wt % MWNT), e) N1i (43 wt % MWNT).	12
Figure 6. FT-IR spectra (KBr) of a) PAni–pTsA, b) N2i (15 wt % CNF), c) N2i (30 wt % CNF), d) N2i (48 wt % CNF), e) N2i (75 wt % CNF).	12
Figure 7. FT-IR spectra (KBr) of a) PAni–pTsA, b) N2i (15 wt % CNF), c) N2i (30 wt % CNF), d) N2i (48 wt % CNF), e) N2i (75 wt % CNF).	13
Figure 8. DC Conductivity (σ_{dc}) and pellet density vs. wt % CNF for nanocomposite N2i synthesized in ethanol.	15
Figure 9. DC Conductivity (σ_{dc}) vs. wt % CNFs for PAni–pTsA coated CNFs (N2i) and PAni–NSA-coated CNFs (N3i).	16
Figure 10. DC Conductivity (σ_{dc}) and pellet density vs. wt % MWNT for nanocomposite N1i (PAni–pTsA coated MWNTs).	17
Figure 11. SEM image of nanocomposite powder particles of N1e (PAni–pTsA ball-milled with MWNT).	18
Figure 12. Plots of DC conductivity (σ_{dc}) vs. wt % MWNTs, PAni–pTsA1, and CNFs.	19
Figure 13. Dielectric spectrum showing ϵ_r' and ϵ_r'' versus X-band microwave frequency for PAni–pTsA1 (9 wt %) in PMMA. ϵ_r' = real permittivity. ϵ_r'' = complex permittivity. ...	20
Figure 14. Dielectric properties of composites PC1i as a function of wt % MWNT. ϵ_r' = real permittivity. ϵ_r'' = complex permittivity. $\tan\delta$ = loss tangent. σ = conductivity.....	22
Figure 15. Dielectric properties of composite PC2i as a function of wt % CNF. ϵ_r' = real permittivity. ϵ_r'' = complex permittivity. $\tan\delta$ = loss tangent. σ = conductivity.....	22

Figure 16. Dielectric properties and conductivities of composite PC3Me (A and B) and PC4Me (C and D). ϵ_r' = real permittivity. ϵ_r'' = complex permittivity. $\tan\delta$ = loss tangent. σ = conductivity.	24
Figure 17. Dielectric properties of composites PC5Me (PAni–NSA mixed with MWNTs ex situ) as a function of wt % MWNT. ϵ_r' = real permittivity. ϵ_r'' = complex permittivity. $\tan\delta$ = loss tangent. σ = conductivity.	25
Figure 18. Dielectric properties of PC6e (PAni–pTsA1 mixed with CNF ex situ) as a function of wt % CNF. ϵ_r' = real permittivity. ϵ_r'' = complex permittivity. $\tan\delta$ = loss tangent. σ = conductivity.	27
Figure 19. Charge transfer complex formation between aniline and the graphitic carbon nanostructure (CNS) surface, and subsequent secondary amine functionalization.	28

List of tables

Table 1. DC conductivity (σ_{dc}) and yields of nanocomposites N2i synthesized in different solvents at various wt % CNF.	14
Table 2. DC conductivity (σ_{dc}) and yields for PAni–pTsA and N2i synthesized at 0 and 25 °C.	14
Table 3. DC conductivity (σ_{dc}) of nanocomposites N1i and N2i synthesized from reaction mixtures subjected to ultrasonication prior to APS addition.	15
Table 4. DC conductivity (σ_{dc}) of doped PAni powders and microwave properties of PAni/PMMA composites (9 wt % PAni) at 10 GHz.	19
Table 5. PMMA composite abbreviations and their components	21
Table 6. Dielectric properties of PMMA composites containing PAni, CNT, and PAni + CNT at 10 GHz	26

Acknowledgements

D.M. would like to acknowledge the support of a DND NSERC for this project.

This page intentionally left blank.

1. Introduction

The focus of this project is to investigate new raw materials for polymer composites with potential for radar absorbing materials (RAM). Traditionally, the active ingredients in RAM are conductive fillers such as metals, carbon fibres, or carbon blacks.^[1,2] More recently, conducting polymers have been investigated for RAM based on their broad-band microwave properties,^[3-22] which are absent in the conductive fillers mentioned above. Carbon nanotube-based materials have also shown good microwave properties for related electromagnetic interference (EMI) shielding applications.^[23-26]

The conductive networks present in RAM are necessary for absorbing microwave frequency electromagnetic (EM) radiation. Incident EM radiation impinging upon a “metallic” surface is dissipated as heat as the electric field component induces electric currents within the conductive material. Broadband microwave absorption can be maximized in combining several resistive layers, such as in a Jaumann absorber.^[27,28]

The overall objective of this work is to investigate novel electronically conductive materials (i.e., PANi–CNT nanocomposites) as potential RAM. These novel raw materials are characterized using FT-IR spectroscopy, SEM and TEM microscopies, dc (static) conductivity (σ_{dc}), and their composites by their σ_{dc} and complex permittivity in the X-band (8-12 GHz).

1.1 Microwave Properties

Microwave properties of materials can be characterized through measurement of the following macroscopic physical properties:

- complex permittivity/dielectric constant (ϵ^*)
- complex permeability (μ^*)
- frequency dependent conductivity
- transmission, absorption, reflection
- EMI shielding effectiveness
- radar cross section (RCS)

The materials discussed in this report were characterized by their conductivity and complex permittivity (ϵ^*) at X-band frequencies (8-12 GHz). The complex permittivity of a material is expressed as

$$\epsilon^* = (\epsilon_r' - i\epsilon_r'')\epsilon_0 \quad (1)$$

When an incident beam of electromagnetic radiation impinges upon a “metallic” surface, the electric field induces electrical currents within the material, which have both capacitive and resistive components.^[29] Capacitive currents generated are 90° out of phase with the applied electric field (AC) voltage, and can be related to the real permittivity (ϵ_r'). Typically, capacitive currents result from polarization due to bound charges or dipoles and can give rise to polarization. The resistive currents also generated within the material arise from free electrons (or metallic states), are in phase with the applied voltage, and give rise to dielectric loss (ϵ_r''). The microwave conductivity σ_{mw} can be calculated from the complex permittivity using the expression:

$$\sigma_{mw} = 2\pi f \epsilon_r'' \epsilon_0 \quad (2)$$

where f is the frequency of incident beam of electromagnetic radiation. For pure electronic conduction, ϵ' should be constant while ϵ'' increases with decreasing frequency f .^[30] Note that

$$\sigma_{mw} = \sigma_{dc} + \sigma_{ac} \quad (3)$$

A useful measure of absorption at microwave frequencies is the loss tangent ($\tan\delta$),^[31]

$$\tan\delta = \epsilon_r'' / \epsilon_r' \quad (4)$$

Materials with $\tan\delta > 1$ are considered lossy materials. $\tan\delta$ values in the order of 10 are considered to indicate strong absorption of radiation at a given frequency.^[31]

1.2 Polyaniline

PAni has received considerable interest for RAM due to the following properties:

- light weight
- environmental stability
- cheap synthesis
- controllable conductivity through doping with various Brönsted acids

PAni exists in several different oxidation states (Figure 1), such as the fully reduced or leucoemeraldine base (PAni-LB), (2) fully oxidized or pernigraniline base (PAni-PB), or the half-oxidized emeraldine base (PAni-EB), which features alternating benzenoid and quinoid repeat units. PAni-EB is the most important form and is relatively insulating, but can be made 9 to 10 orders of magnitude more conductive upon protonation of the imine nitrogens with suitable acids to give the emeraldine salt (PAni-ES, Figure 1); a process known as chemical doping.

The main drawbacks with PAni-ES are the low solubility, infusibility, and intractability as a solid, which makes processing relatively difficult. Furthermore PAni-ES alone has poor mechanical properties due to its rigid polymer backbone. Despite the drawbacks, many

conductive PANi-ES composites with low percolation thresholds (p_c) have been reported in polymer blends/composites.^[32,33]

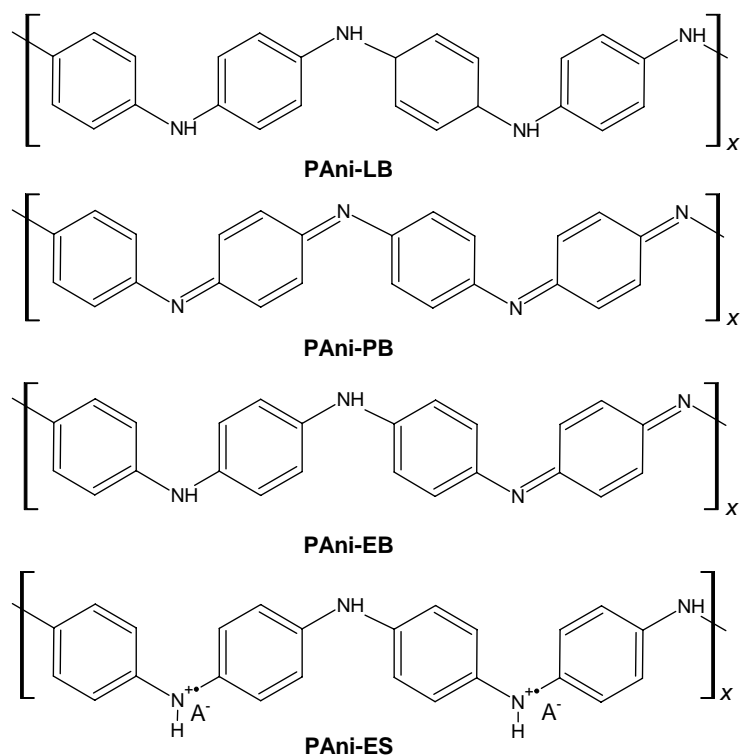


Figure 1. Repeating structures of various forms of Polyaniline.

1.3 Carbon Nanotubes

Carbon nanotubes are tubular sheets of graphite available as single or multiwalled structures (SWNTs or MWNTs, respectively) and are well known for their excellent intrinsic electrical, thermal, and mechanical properties.^[34,35] CNTs are insoluble, highly intractable, and infusible solids, which makes processing into a useful form difficult. CNTs are also difficult to disperse in liquids because their structures are mechanically entangled and highly bundled due to strong van der Waals interactions. This poses a major challenge for producing usable materials.^[36] CNTs are also commercially expensive, mainly because of the difficulty in producing CNTs in high purity and with as few structural defects as possible. Considerable effort has been invested by several research groups to improve the processibility of CNTs through both covalent^[37-41] and noncovalent^[42-45] surface modification. Despite the drawbacks, several successful attempts have produced CNT/polymer composites, which show good conductivity at low loading.^[44-49]

1.4 Polyaniline–Carbon Nanotube Nanocomposites

A promising theme that has developed recently is the formation of CP/CNT nanocomposites by combining CPs such as PANi,^[50-66] polypyrrole (PPy),^[67-71] poly(3-octylthiophene),^[72] polyethylene dioxythiophene (PEDOT),^[73] poly(*p*-phenylene vinylene),^[74,75] and poly{*m*-phenylenevinylene)-*co*-[(2,5-dioctyloxy-*p*-phenylene)vinylene]}^[76-80] with SWNT or MWNTs. Synergistic effects between CP and CNT have been proposed to result in materials with enhanced properties over their individual constituents. This synergistic effect should arise from multiple interactions between the CNT surface and the CP backbone. The high conductivity and aspect ratio of CP/CNT nanocomposites dispersed in an insulating polymer matrix should give a composite with improved electrical, thermal, and mechanical properties.

Several research groups have reported the synthesis of PANi-coated CNT nanocomposites (PANi–CNT) and their various physical properties.^[50-53,55-66,81] The first PANi–CNT reported was produced by electrochemical polymerization of aniline onto CNT electrodes.^[62,65,66] Cochet and coworkers were the first to chemically polymerize PANi onto multiwalled nanotubes (MWNTs) to give nanocomposites with enhanced electrical properties.^[64] Others have reported conductivity enhancements of up to 25-fold at as low as 10 wt % CNTs.^[55-57,59,61,64,82] Wei and coworkers used sulfonated MWNTs (MWNT–(OSO₃H)) to dope PANi-EB.^[83] The conductivities for PANi–MWNT–(OSO₃H) nanocomposites were significantly higher than for undoped PANi-EB at low MWNT–(OSO₃H) loading.^[83] The electrical properties of PANi–CNT relative to the individual components are likely highly dependent on the quality of the CNTs used as well as dopant and degree of doping of the PANi coating. Related nanocomposites with substituted PANi and CNTs,^[50,60] as well as PANi and graphite^[56] or carbon nanofibres (CNFs)^[63,84] have also been reported.

For this report, we wanted to: (1) investigate the feasibility of the synthesis of new PANi–CNT and PANi–CNF conductive nanocomposites, (2) investigate processing PANi, CNTs, CNFs, PANi–CNT, PANi-coated CNFs (PANi–CNF) separately into usable forms to (3) investigate if synergistic effects between PANi and CNTs/CNFs can give composites with enhanced microwave properties (i.e., X-band complex permittivity) over composites containing their individual constituents. (1) has already been accomplished (*vide supra*). Regarding (2), conductive composites containing PANi–CNT or PANi–CNF nanocomposites as filler have not been reported. Finally, the microwave properties of PANi–CNT or PANi–CNF materials have not been explored.

2. Experimental

2.1 Synthesis

2.1.1 Polyaniline

Doped PANis were synthesized using the well known chemical oxidative polymerization procedure using ammonium persulfate (APS).^[85] The ratio of aniline : APS was fixed at 1 : 1 (47.0 mM each). The sulfonic acids *para*-toluene sulfonate (pTsA), 2-naphthalene sulfonic acid (NSA), *para*-dodecylbenzenesulfonic acid (DBSA), 2,5-naphthalenedisulfonic acid (NDSA), and benzenesulfonic acid (BSA) were used as dopants (1 M), because their salts with PANi possess good conductivity and are thermally stable. Water or ethanol (95 %) were used as the reaction solvents. Reactions were conducted in closed containers under ambient conditions or in an environmental chamber (Tenney) between 0-5 °C.

2.1.2 Polyaniline–Multiwalled Nanotube/Polyaniline–Carbon Nanofibre Nanocomposites

Nomenclature:

- N1i - PANi-pTsA coated MWNT nanocomposites (*in situ*)
- N2i - PANi-pTsA coated CNFs (*in situ*)
- N3i - PANi-NSA coated CNFs (*in situ*)
- N1e - PANi-pTsA mixed with MWNTs (*ex situ*)
- N2e - PANi-pTsA mixed with CNFs (*ex situ*)

“*In situ*” method: Nanocomposite N1i was prepared similarly to nanocomposites from a reported *in situ* polymerization procedure.^[64] For this work, reactions were conducted in both water and ethanol; the latter was preferred because MWNTs and CNFs dispersed better in that medium. A representative example of a synthesis is as follows. pTsA (4.78 g, 25.1 mmol) and aniline (150 μ L, 1.65 mmol) were dissolved in ethanol (30 mL). MWNTs (30-100 mg, from Aldrich : 95 %, diam. = 20 - 50 nm, length = 5 - 20 μ m) were then added to the solution with stirring. The mixture was sonicated in an ultrasonic bath (12 W and 55 kHz or 100 W and 47 kHz) for at least 5 min and then cooled to 0 °C. A precooled solution of APS (369 mg, 1.62 mmol) in 5 mL ethanol : water (3 : 2) was then added and the reaction was stirred for ~20 h. The reaction mixture was then filtered using a medium porosity glass frit and thoroughly washed with ethanol and acetone until each filtrate was colorless to give a dark green/black powder, which was dried *in vacuo* for 24 h.

N2i powders were prepared using the “*in situ*” method, except that MWNTs were replaced with CNFs (Pyrograf Products Inc., P-II, grade RR-24-PS-LD, batch #130).

N3i powders were prepared using the “*in situ*” method, except that NSA was used instead of pTsA.

Note that for N1i, N2i, and N3i the wt % MWNT or CNF in the final product was calculated under the assumption that no loss of MWNT or CNF mass occurred during the workup.

“*Ex situ*” method: Nanocomposites N1e and N2e were prepared by dry mixing PANi-ESs with MWNTs or CNFs with one acrylic ball in a polystyrene vial using a ball-mill for 30 min.

2.2 Poly(methyl methacrylate) Composites

PMMA (Buehler transoptical powder) and hydroquinoneⁱⁱ were mixed with the conductive filler(s) (i.e., MWNTs, CNFs, N1a, or N2a) with an acrylic ball in a polystyrene vial via ball-milling for 30 min. The visually homogeneous powders obtained were then transferred into the loading chamber of a Buehler mounting press equipped with a heating mantle, compressed to 80 psi., and heated for 30 min. During this time, the temperature was monitored using a thermocouple to change from room temperature to ~145 °C. After 30 min, the heating mantle was removed and replaced with a water condenser to cool the samples enough to be removed as rigid, plastic disks, which were then carefully machined to the dimensions of a rectangular X-band waveguide (10.16 × 22.86 mm).

2.3 Fourier Transform-Infrared Spectroscopy

IR spectra were recorded using a Nicolet Nexus 670 Fourier Transform-Infrared (FT-IR) spectrometer.

2.4 Electron Microscopy

Samples for scanning electron microscopy (SEM) images were gold sputter-coated and imaged using a JEOL LEO 1455VP instrument. Samples for transmission electron microscopy (TEM) images were deposited onto holey carbon coated copper grids and imaged using a Hitachi H-7000 instrument.

2.5 Conductivity Measurements

The DC conductivity (σ_{dc}) of PANi, MWNT, CNF, nanocomposites N1i, N2i, N1e, and N2e powders were determined on 13 mm compressed pellets (15 psi for 1 min) using a Jandel four-point probe (gold probes spaced 1 mm apart). Current was applied through the outer probes from a Hewlett-Packard 6224B voltage supplier and was measured with a Hewlett-

ⁱⁱ Hydroquinone was added to plasticize PANi.

Packard 34401A multimeter. The voltage drop was measured between the two inner probes using a Fluke 8000A multimeter.

σ_{dc} for PMMA composites could not be determined using the four point probe method because of high contact resistances. Therefore, σ_{dc} was determined by applying silver paint to the short ends of the rectangular samples and measuring the resistance (R) down the length of the sample between them. The dc conductivity (σ_{dc}) down the length of each sample was calculated using the equation:

$$\sigma_{dc} = L/R \times A$$

where, A is the area of each silver paint electrode (in cm^2). The σ_{dc} values obtained were accepted as true values based on the agreement with the microwave conductivity (σ_{mw}) values at 10 GHz.

2.6 Permittivity Measurements

Reflectivity measurements from 8 to 12 GHz were made using an HP8720C vector network analyzer. The real and imaginary components of the permittivity were determined from the S11 and S21 parameters using a procedure similar to a recently reported modified transmission-reflection method.^[86]

3. Results and Discussion

3.1 Synthesis

Polyanilines (PANis) were synthesized by a standard literature procedure involving the chemical polymerization of aniline in acidic solution (water or ethanol) in the presence of the initiator ammonium persulfate (APS).

Four classes of nanocomposites were prepared: N1i, N2i, N1e, and N2e (refer to section 2.1.2 for nomenclature). Nanocomposites N1i and N2i were prepared via the *in situ* polymerization of aniline in the presence of CNFs and MWNTs, respectively. Nanocomposites N1b and N2b were prepared via the *ex situ* mixing of PANi-pTsA2 powder with CNF and MWNT powders respectively. *Ex situ* mixing was accomplished via ball-milling the dry powders together for 30 min. N1a, N1b, N2a, and N2b were all prepared at varied ratios of PANi : CNF or MWNT.

3.2 Microscopy

The presence of a PANi coating in nanocomposites N1i and N2i was observed using transmission electron microscopy (TEM) and scanning electron microscopy (SEM). N1i and N2a are more easily distinguished from uncoated CNT and CNFs, respectively, by TEM. TEM images clearly show a PANi sheath coating the MWNTs (Figure 3b) and CNFs (Figure 3d), which is absent on the uncoated structures (Figures 3a and c, respectively). Qualitatively, the uniformity and thickness of the PANi coatings appeared to depend on the wt % CNT and CNFs used in the reactions. In Figure 3b, the diameter of the PANi coating appears to be twice that of the embedded NT. SEM images also qualitatively show that N1i and N2i are slightly thicker and have a rougher surface appearance compared to uncoated CNT and CNFs (Figure 2). The absence of loose particulate in N1i and N2i suggests that the increased mass of the CNT and CNFs after subjecting to *in situ* polymerization is due to a PANi coating. No significant change in mass was recorded when CNT and CNFs were subjected to the reaction conditions without aniline, ruling out a change in mass due to anything but PANi.

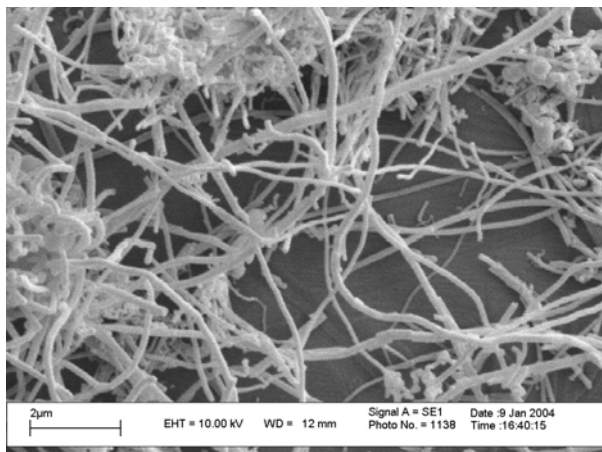
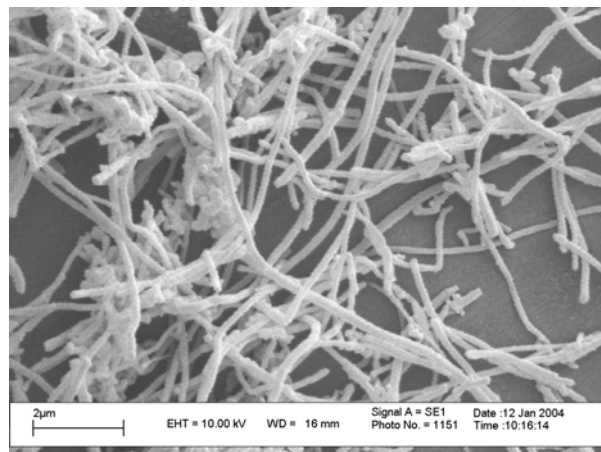
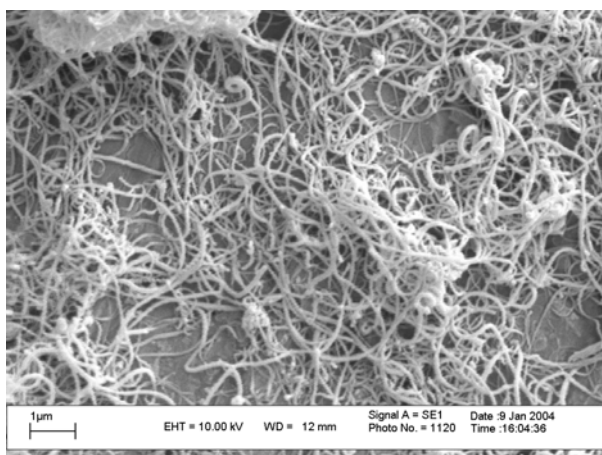
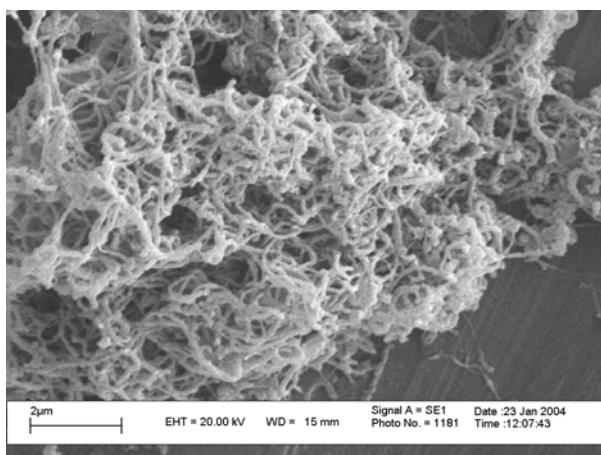
A**B****C****D**

Figure 2. SEM images of a) uncoated CNFs, b) nanocomposite N1i, c) uncoated MWNTs, and d) nanocomposite N2i.

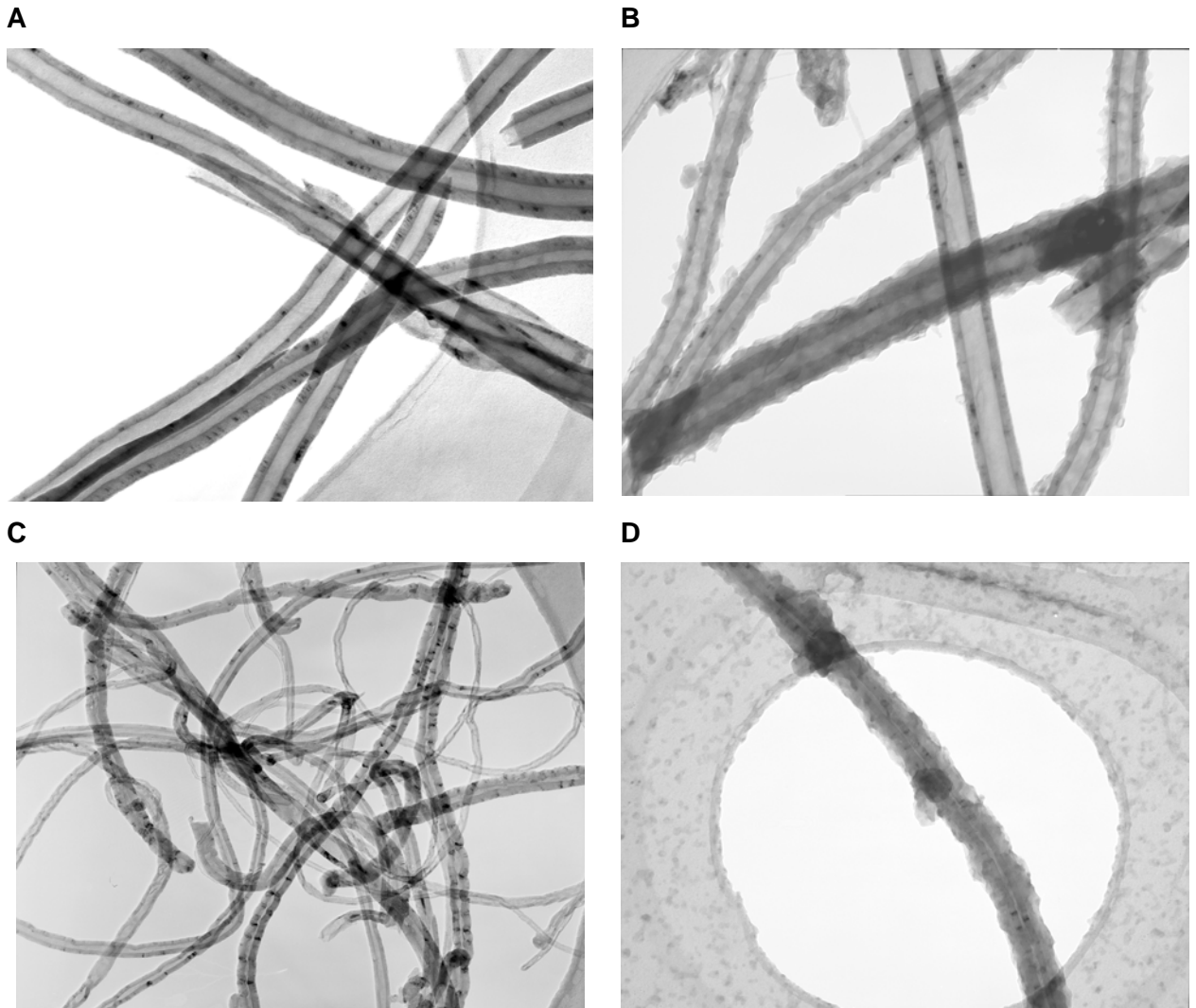


Figure 3. TEM images of a) *uncoated CNFs*, b) *nanocomposite N1i*, c) *uncoated MWNTs*, d) and *nanocomposite N2i*.

3.3 Fourier Transform-Infrared Spectroscopy

FT-IR spectra were recorded on the N1i (Figures 5) and N2i (Figures 6 and 7) synthesized in this study to probe potential interactions between the PANi coating and carbon.

All nanocomposite samples showed typical absorptions attributable doped PANi–pTsA:

- 3202, 3071 cm^{-1} (N–H str.)
- 1606, 1577 cm^{-1} (N=Q=N ring str)ⁱⁱⁱ
- 1465 cm^{-1} (N–B–N ring str),
- 1301 cm^{-1} (Q=N–B str.)
- 1156 cm^{-1} (N=Q vib.)
- 1122 cm^{-1} (C–H bend)
- 875 cm^{-1} (C–H bend)
- 813 and 795 cm^{-1} (C–H bend)
- 677 cm^{-1} (C–C bend)
- 1030, 1006 cm^{-1} (S=O str).

In addition, previously reported interactions between the PANi backbone and CNT and CNFs were also observed for N1i and N2i.^{[59],[58]} First, a strong broad signal near 3400 cm^{-1} is present for both N1i (Figure 5) and N2i (Figure 7), which is absent in the spectrum for PANi–pTsA alone (Figures 5a, 6a, and 7a). Signals in this region have been observed previously and are speculated to arise from charge transfer interactions between the PANi N–Hs and MWNTs.^[59] A signal located at ~1240 cm^{-1} for PANi–ES, normally attributed to $\text{C}_{\pi}\cdots\text{N}$, increased in relative intensity with increasing wt % MWNT and CNFs. Also a new signal emerged at 1220 cm^{-1} , which is absent for PANi alone. Baibarac and coworkers have previously attributed these signals to $\text{C}-\text{N}^+$ stretching in proposed structures 1 and 2, respectively (Figure 4).^[58] Finally, the relative intensities of the sharp signals at ~1122–1156 cm^{-1} also increase with wt % CNF or MWNT. These signals are normally attributed to a mode of $\text{Q}=\text{N}^+\text{H}-\text{B}$ or $\text{B}-\text{NH}-\text{B}$ stretching.^[58]

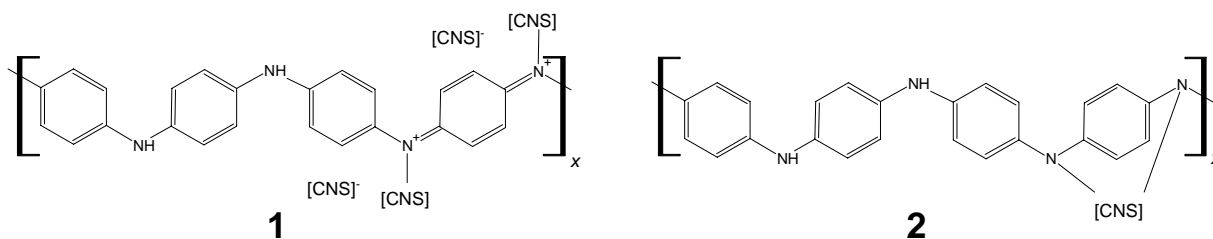


Figure 4. Possible Polyaniline–carbon nanostructure complex structures (carbon nanostructures (CNS)= carbon nanotubes or carbon nanofibres).

ⁱⁱⁱ Q = Quinoid. B = Benzenoid

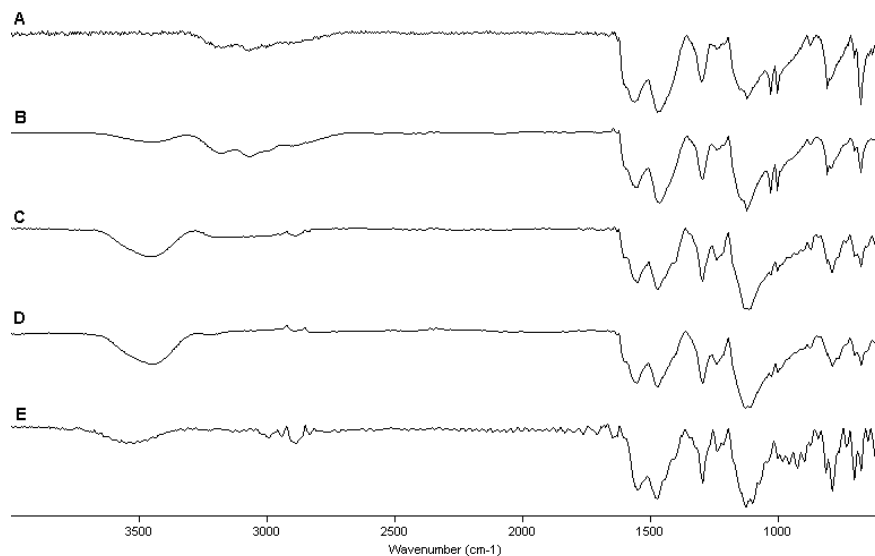


Figure 5. FT-IR spectra (KBr) of a) PANi-pTsA, b) N1i (8 wt % MWNT), c) N1i (19 wt % MWNT), d) N1i (27 wt % MWNT), e) N1i (43 wt % MWNT).

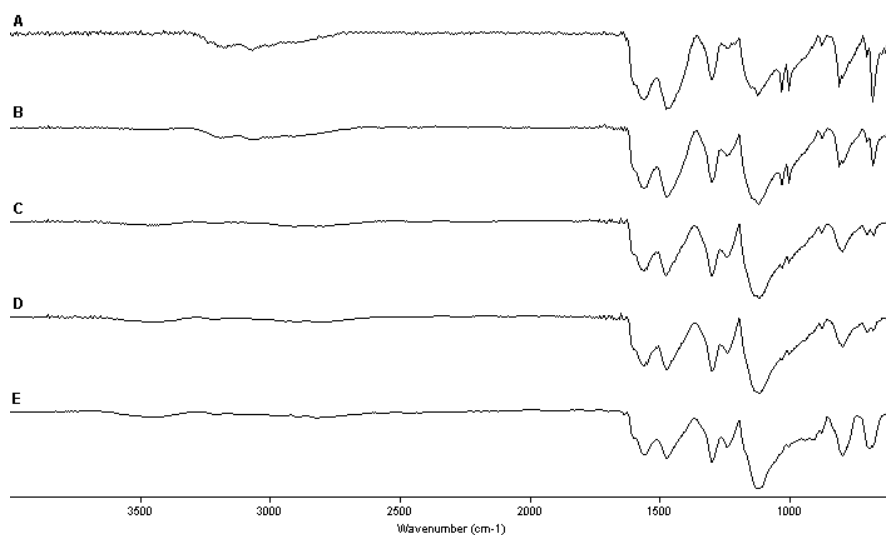


Figure 6. FT-IR spectra (KBr) of a) PANi-pTsA, b) N2i (15 wt % CNF), c) N2i (30 wt % CNF), d) N2i (48 wt % CNF), e) N2i (75 wt % CNF).

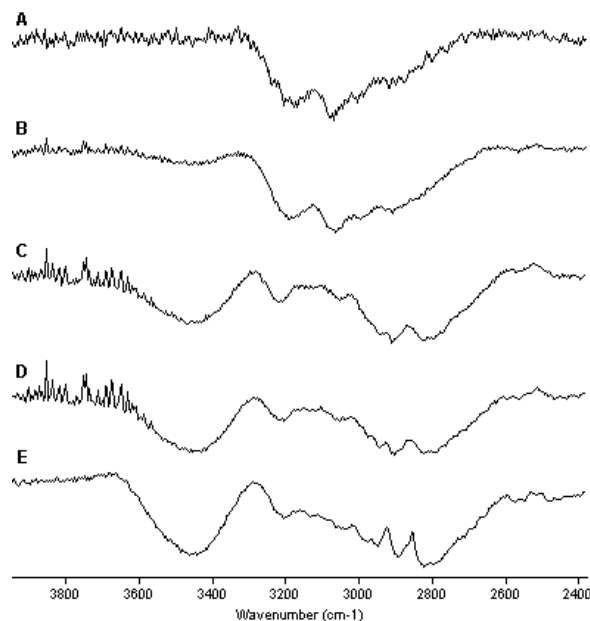


Figure 7. FT-IR spectra (KBr) of a) PAni-pTsA, b) N2i (15 wt % CNF), c) N2i (30 wt % CNF), d) N2i (48 wt % CNF), e) N2i (75 wt % CNF).

3.4 The DC Conductivity of Bulk Polyaniline–Carbon Nanofibre Nanocomposites

Several synthetic parameters for N1i and N2i were adjusted to obtain products with the highest possible conductivities. Most of the preliminary work was conducted for N2i, because CNFs are less expensive than MWNTs. We hoped that a changes to the synthetic conditions for the formation of N2i would have a similar effect in the formation of N1i, since MWNTs and CNFs have some structural similarities; both possess graphite surfaces. *In situ* chemical oxidative polymerization of aniline in the presence of CNFs was carried out using a procedure similar to previous reports using APS.^[87] pTsA and NSA were used as the dopants because of their interesting microwave absorption properties (*vide infra*). Ethanol was preferred over water as the solvent because CNFs dispersed better in ethanol, and reactions in ethanol furnished more conductive products in higher yield (Table 1). Reactions were run at 0 °C because more conductive products in higher yields were obtained (Table 2).

Table 1. DC conductivity (σ_{dc}) and yields of nanocomposites N2i synthesized in different solvents at various wt % CNF.

wt % CNF	σ_{dc} (S/cm)		yield (mg)	
	water	ethanol	water	ethanol
30	10.5	13.2	165.0	182.9
60-65	17.2	29.5	313.1	333.3
75-79	16.9	31.9	500.1	541.4

N2i = PANi-coated CNFs.

Table 2. DC conductivity (σ_{dc}) and yields for PANi-pTsA and N2i synthesized at 0 and 25 °C.

	CNF (mg)	T (°C)	σ_{dc} (S/cm)	yield (mg)
PANi-pTsA	-	0	2.6	164.3
PANi-pTsA	-	25	1.6	74.5
N2i	104.8	0	19.3	222.4
N2i	106.3	25	15.9	197.5

N2i = PANi-coated CNFs.

The untreated CNFs (and MWNTs) used in this study exist as mechanically entangled masses. CNFs are very hydrophobic, which leads to aggregation in polar media such as ethanol or water due to strong van der Waals interactions. Therefore, to get a uniform PANi surface coating, CNFs and MWNTs have to be sufficiently dispersed in the reaction medium. This can be done using an ultrasonic bath.^[36] The dispersion and fracture of solids in a liquid medium subjected to ultrasonication occurs via cavitation, which is the formation and implosion of tiny vacuum bubbles. Lower ultrasonic frequencies produce larger bubbles, which collapse more violently and are more destructive. In this study, CNFs (and MWNTs) were dispersed in water or ethanol using an ultrasonic bath for varied lengths of time and at different frequencies (55 kHz and 47 kHz).

The effect of sonication time prior to APS addition on σ_{dc} values for N1i and N2i is shown in Table 3. For N2i, sonication times between 5 and 360 min did not have a significant impact on σ_{dc} . σ_{dc} decrease very little after longer times (Table 3). Sonication time also doesn't appear to have a significant impact on the σ_{dc} for N1i. Based on σ_{dc} data alone, sonication time and frequency an insignificant impact on product formation and σ_{dc} .

Table 3. DC conductivity (σ_{dc}) of nanocomposites N1i and N2i synthesized from reaction mixtures subjected to ultrasonication prior to APS addition.

	time (min)	σ_{dc} (S/cm)	
		55 kHz	47 kHz
N2i	5	19.3	-
N2i	60	20.4	-
N2i	180	20.7	26.2
N2i	360	16.7	21.5
N1i	5	18.4	-
N1i	180	18.4	-

N1i = PANi-coated MWNTs, N2i = PANi-coated CNFs.

Figure 8 shows σ_{dc} of PANi-pTsA nanocomposites synthesized with varying wt % CNF under the same conditions. σ_{dc} increases linearly with wt % CNF to values significantly exceeding the two individual components; i.e., ~10 times greater than PANi-pTsA and ~30 times greater than CNF alone. This behaviour is interesting and does suggest synergy between the PANi and CNFs.

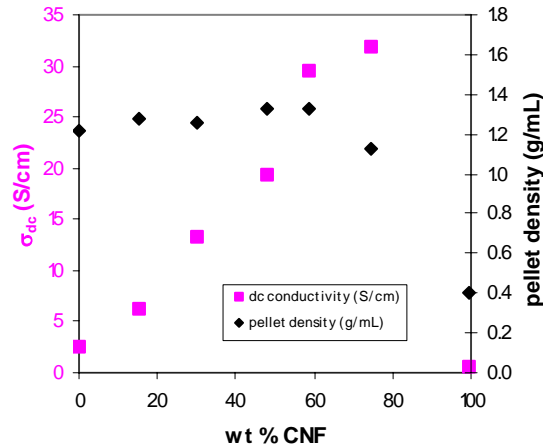


Figure 8. DC Conductivity (σ_{dc}) and pellet density vs. wt % CNF for nanocomposite N2i synthesized in ethanol.

Nanocomposites N2e were also prepared by *ex situ* mixing of PANi-pTsA and CNF powders (section 2.1.2). In contrast to N2i pellets, N2e pellets containing a 1 : 1 ratio of PANi-pTsA : CNF displayed much lower conductivity and mechanical stability, making σ_{dc} measurements

difficult. Physical interactions between the PANi–pTsA coating and the pi-conjugated surface of the CNFs may be contributing to the increase in σ_{dc} for the *in situ* product, N2i.

PAni–NSA-coated CNFs were also synthesized by *in situ* polymerization. It is well known that the conductivity of doped PANis are influenced the type of acid dopant.^[88,89] Figure 9 compares σ_{dc} for N2i and N3i nanocomposites as a function of wt % CNF. Both sets of data are nearly superimposable and may suggest that the increase in σ_{dc} observed for N2i is independant of the dopant used.

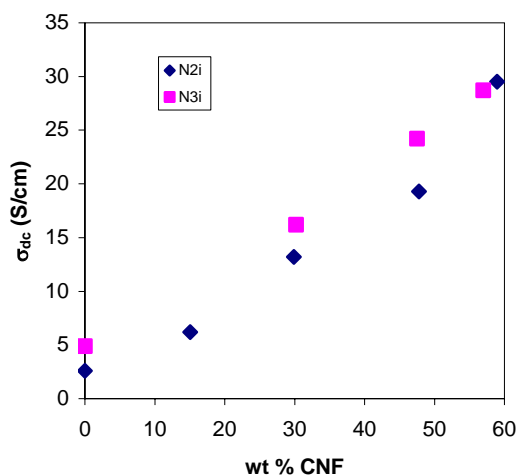


Figure 9. DC Conductivity (σ_{dc}) vs. wt % CNFs for PANi–pTsA coated CNFs (N2i) and PANi–NSA-coated CNFs (N3i).

3.5 The DC Conductivity of Polyaniline–Multiwalled (Carbon) Nanotube Nanocomposites

Figure 10 shows σ_{dc} data for N1i containing various wt % MWNT. σ_{dc} increases linearly with wt % MWNT, exceeding the values of PANi–pTsA or MWNT alone. At 60 wt % MWNT, N1i is nearly 30 times more conductive than PANi synthesized under the same conditions and ~4 times more than MWNT. Note that relatively low MWNT loading (i.e., ~20 %) gives a significant increase (10-fold) in conductivity relative to PANi–pTsA. This behaviour is clearly different from the percolation behaviour reported for a poly(*m*-phenylenevinylene)-*co*-[(2,5-dioctyloxy-*p*-phenylene)vinylene]–CNT nanocomposite; a significant rise over a small change in wt % CNT to a maximum value at a plateau was observed.^[90]

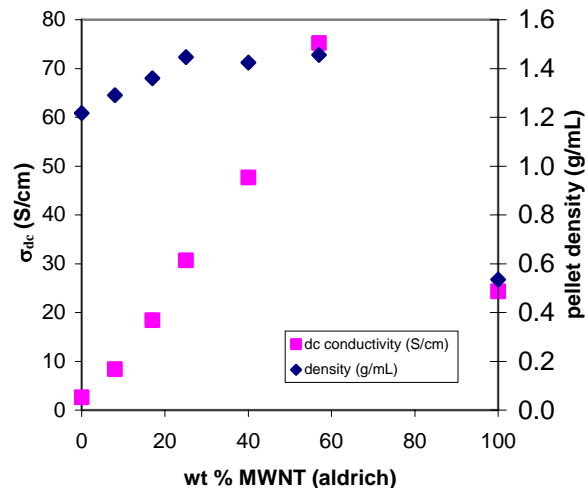


Figure 10. DC Conductivity (σ_{dc}) and pellet density vs. wt % MWNT for nanocomposite N1i (PAni-pTsA coated MWNTs).

Nanocomposites N1e were also prepared by *ex situ* mixing of PAni-pTsA and MWNT powders at varied ratios (see section 2.1.2). Examination of the nanocomposite powders N1e by SEM showed MWNT fragments adsorbed to the surface of the much larger PAni-pTsA particles (Figure 11). The nanocomposites N1e were more conductive than PAni-pTsA, but not bulk MWNTs. For example, at 30 wt % MWNT, σ_{dc} was ~20 S/cm, which is lower than the *in situ* nanocomposite N1i at the same wt % MWNT (Figure 10). Furthermore, at high wt % MWNTs (>40 %), nanocomposite pellets were brittle and difficult to keep intact, which was not the case for pellets of the *in situ* material. Thus, *in situ* coating appears to furnish a nanocomposite powder with greater bulk σ_{dc} and mechanical properties.

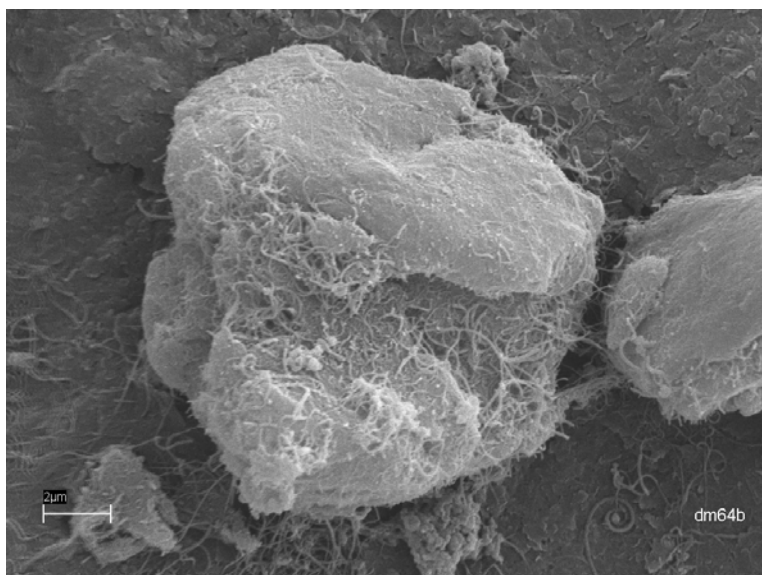


Figure 11. SEM image of nanocomposite powder particles of N1e (PAni-pTsA ball-milled with MWNT).

The enhanced σ_{dc} for N1a and N2a with increasing wt % carbon clearly is not characteristic of a percolative network, but is more like a semi-interpenetrating network (SIPN).

Interpenetrating networks characteristically show a more gradual rise in conductivity over a greater range of wt % conductive component, which is also accompanied by an increase in material density.^[91] For nanocomposites N1i and N2i, less conductive PAni effectively interpenetrates the voids within the network of CNFs and MWNTs. The PAni coating probably helps reduce contact resistance between the intrinsically more conductive CNFs and MWNTs by facilitating inter-tube/fibre electron transport relative to void spaces of air in the absence of PAni.

3.6 Poly(methyl methacrylate) Composites

Neither PAni nor MWNTs alone are suitable for coatings materials due the poor mechanical properties of each bulk solid. A common way of processing PAni or MWNT into a usable form is to incorporate them into another insulating polymeric matrix at a concentration low enough to result in a composite that improves one physical property of the final composite, i.e., conductivity, without significantly degrading the properties of the matrix polymer (i.e., mechanical properties).^[32,33,44-49] A wide range of matrix polymers have been used for both PAni and MWNT composites. PMMA is a good insulating matrix for PAni^[92-105] and CNT^[106-109] composites and has good mechanical properties and high transparency. We determined $\sigma_{dc} < 2.2 \times 10^{-7}$ S/cm, $\epsilon_r' = 2.6$, $\epsilon_r'' = 0.12$, and $\tan \delta = 0.046$ for PMMA.

PMMA composites were produced using a procedure similar to a literature report (see section 2.2).^[92] PAni and MWNT could be incorporated into PMMA easily by powder mixing and melt processing to yield conductive composites with low percolation thresholds (p_c). That is, conducting networks within the PMMA samples form at low wt % of conductive filler. We

found p_c s for PANi and MWNT were less than 1 % (Figure 12). p_c for CNFs in PMMA was found to be significantly higher (i.e., could be at least 10 %).

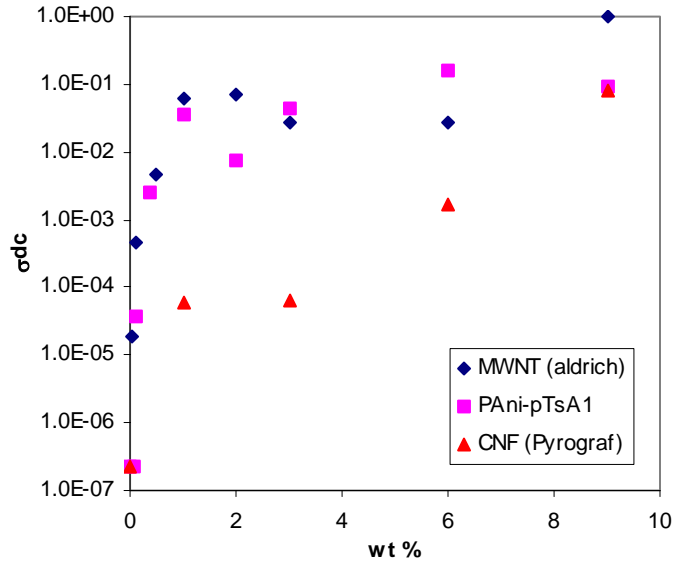


Figure 12. Plots of DC conductivity (σ_{dc}) vs. wt % MWNTs, PANi-pTsA1, and CNFs.

Table 4 lists the microwave properties determined for various PMMA composites containing PANis with different dopants (9 wt %). PANi-pTsA and NSA polymers were chosen for further studies with MWNTs and CNFs because they gave the most lossy PMMA composites (Table 4). Note that PANi-pTsA1 and 2 are different batches synthesized under the same conditions.

Table 4. DC conductivity (σ_{dc}) of doped PANi powders and microwave properties of PANi/PMMA composites (9 wt % PANi) at 10 GHz.

dopant (1 M)	σ_{dc} pellet (S/cm)	σ_{dc} PMMA composite (S/cm)	σ_{mw} (10 GHz) PMMA composite (S/cm)	ϵ_r''	ϵ_r'	$\tan \delta$
pTsA1	2.3	0.0950	0.100	17.8	13.0	1.4
pTsA2	3.6	0.0500	0.220	39.4	11.7	3.4
NSA	6.6	0.2200	0.130	23.3	11.8	2.0
DBSA	1.3	-	0.012	2.3	7.2	0.3
BSA	4.4	0.0010	0.065	11.6	10.4	1.1
NDBSA	0.5	0.0002	0.016	6.3	2.8	0.5

σ_{mw} = microwave conductivity. ϵ_r'' = imaginary permittivity. ϵ_r' = real permittivity. $\tan \delta$ = loss tangent. pTsA = para-toluene sulfonic acid. NSA = 2-naphthalene sulfonic acid. DBSA = 4-dodecylbenzene sulfonic acid. BSA = benzene sulfonic acid. NDBSA = 1,5-naphthalenedisulfonic acid. pTsA1 and pTsA2 are different batches synthesized under the same conditions.

Figure 13 shows a representative dielectric spectrum of PANi/PMMA composites. For all samples, both ϵ_r' and ϵ_r'' were observed to decrease with increasing frequency from 8-12 GHz.

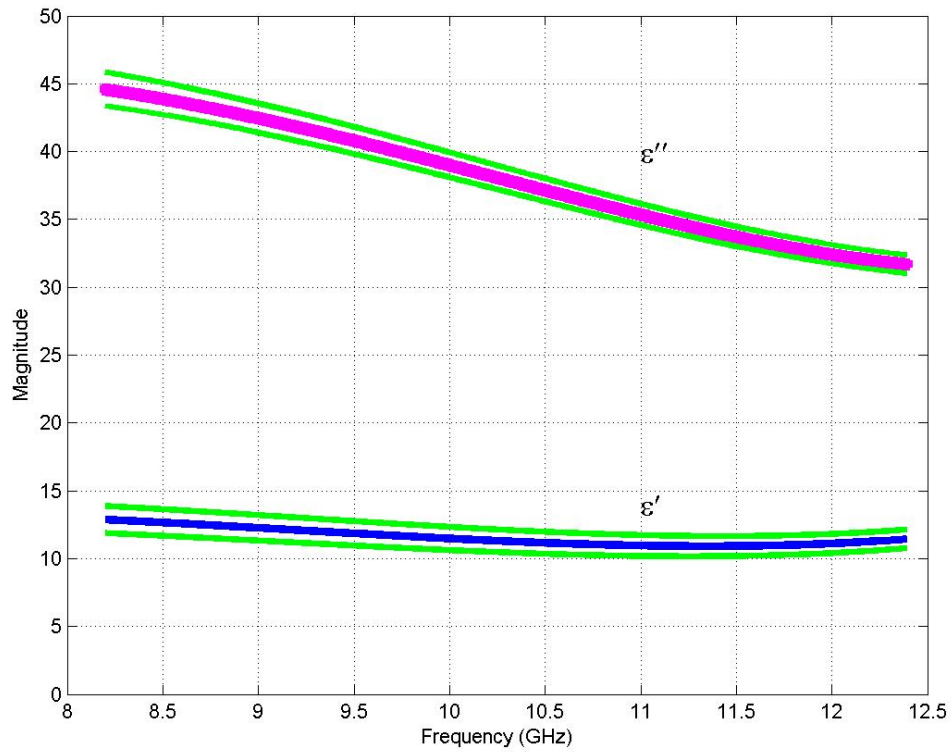


Figure 13. Dielectric spectrum showing ϵ_r' and ϵ_r'' versus X-band microwave frequency for PANi-pTsA1 (9 wt %) in PMMA. ϵ_r' = real permittivity. ϵ_r'' = complex permittivity.

Table 5 lists the PMMA composites incorporating PAni, MWNTs and CNFs. Each varies in the type of conductive filler present in the insulating PMMA matrix. The total amount of conductive filler was set at 9 % for all composites. For samples containing two conductive components the ratio of each was varied while maintaining a total of 9 wt % overall (i.e. for PC1Me, PC2Me, PC3Me, and PC15e).

Table 5. PMMA composite abbreviations and their components

Name	Conductive Filler(s)
PC1i	N1i (PAni-pTsA coated MWNTs)
PC2i	N2i (PAni-pTsA coated CNFs)
PC3Me	PAni-pTsA1, MWNT
PC4Me	PAni-pTsA2, MWNT
PC5Me	PAni-NSA, MWNT
PC6e	PAni-pTsA1, CNF

All PMMA composites contained ~7.5 wt % hydroquinone. The total amount of conductive filler in each composite was 9 wt %. PAni = Polyaniline, pTsA = para-toluene sulfonic acid, NSA = naphthalene sulfonic acid, MWNT = multiwalled (carbon) nanotubes, CNF = carbon nanofibres, N1a = PAni-pTsA coated MWNTs (*in situ*), N2a = PAni-pTsA coated CNFs (*in situ*). Note that PAni-pTsA1 and PAni-pTsA2 are two different batches of PAni-pTsA.

σ , ϵ_r'' , and $\epsilon_r'^{iv}$ were all found to change with increasing wt % MWNT or CNFs for PC1i (Figure 14) and PC2i (Figure 15), respectively. Microwave absorption reaches a minimum near 1 : 1 PAni : MWNT as σ_{dc} , ϵ_r'' , and $\tan\delta$ all reach minimum values. Composites PC1i are poorer microwave absorbers than PAni-pTsA/PMMA or MWNT/PMMA composites, despite the fact that the σ_{dc} s of the fillers N1i or N2i are higher than PAni-pTsA or MWNT (*vide supra*). The observed behaviour is less surprising for N2i because CNF/PMMA composites are relatively poor microwave absorbers compared to PAni-pTsA/PMMA or MWNT/PMMA.

^{iv} Note the increase for ϵ_r' with increasing wt % MWNT all PMMA composites. Increasing capacitive effects between neighbouring MWNTs in the PMMA matrix may be one explanation for this. Similar effects have been previously suggested to be due to the increased concentration point defects on the CNT surfaces (see reference 21). More defects will be present at higher CNT loadings.

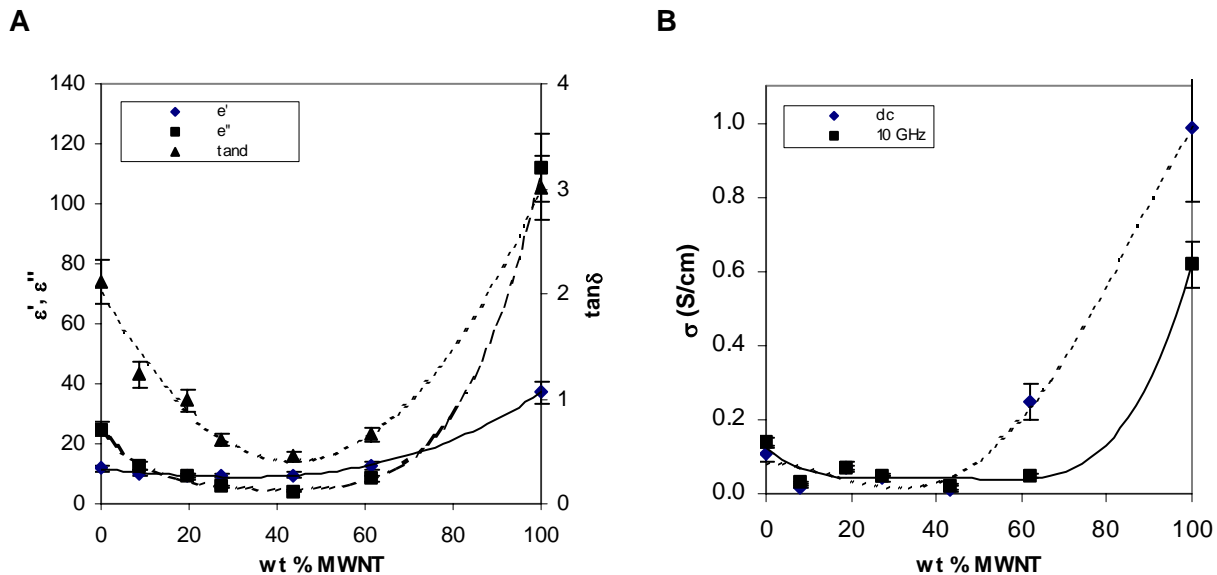


Figure 14. Dielectric properties of composites PC1i as a function of wt % MWNT. ϵ_r' = real permittivity. ϵ_r'' = complex permittivity. $\tan\delta$ = loss tangent. σ = conductivity.

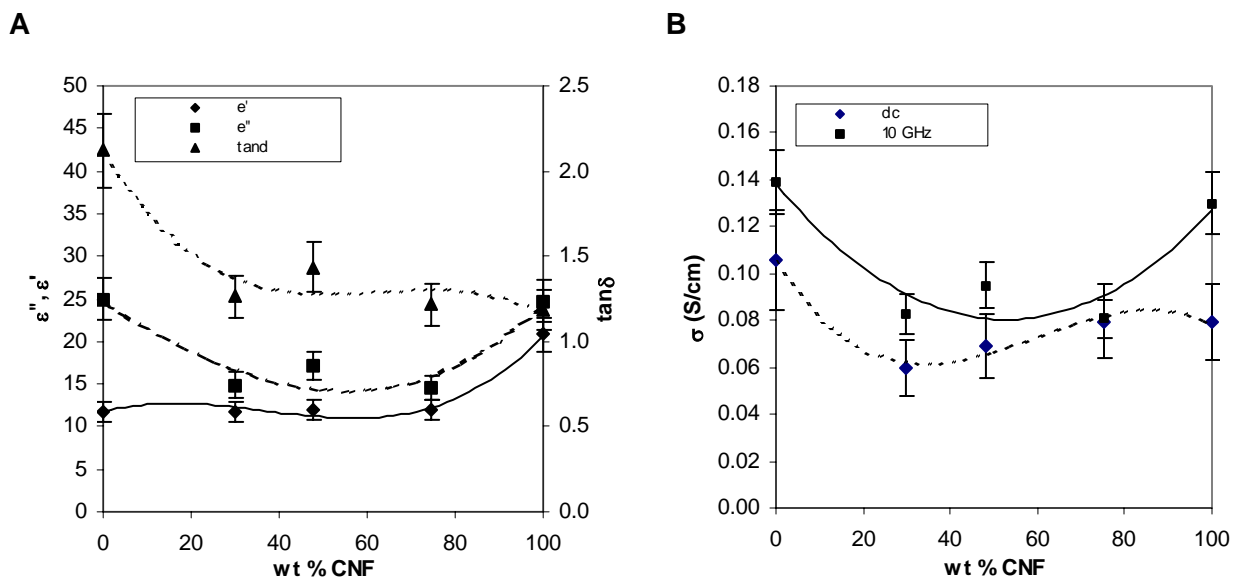


Figure 15. Dielectric properties of composite PC2i as a function of wt % CNF. ϵ_r' = real permittivity. ϵ_r'' = complex permittivity. $\tan\delta$ = loss tangent. σ = conductivity.

The poor microwave absorption by PC1i and PC2i is probably due to poorer processability (high p_c) relative to PMMA composites containing PANi-pTsA or MWNT alone. Coated MWNTs (or CNFs) may be less compatible with PMMA. Poor dispersion of the fillers N1i and N2i in PMMA may be because these powders are more difficult to break down into

primary particles. Incompatibility with PMMA may cause the PANi coated MWNT and CNF particles to agglomerate in the melt to the extent where percolation networks have significantly decomposed and gross phase separation occurs.

The dielectric properties and conductivities of PMMA composites containing PANi-pTsA and MWNTs mixed *ex situ* (i.e., PC3Me and PC4Me in Table 5) at 9 wt % total conductive filler and varied ratios of PANi : MWNT are shown in Figure 16. Note that in contrast to composites PC1i and PC2i, PANi and MWNT were combined *ex situ* (see experimental section 2.1.2). Composites PC3Me and PC4Me showed improved microwave absorption properties relative to PANi-pTsA(1 or 2)/PMMA or MWNT/PMMA composites. σ_{dc} , ϵ_r'' , and ϵ_r' all increase with increasing wt % MWNTs, while $\tan\delta$, reaches a maximum when PANi : MWNT is near 1 : 1.

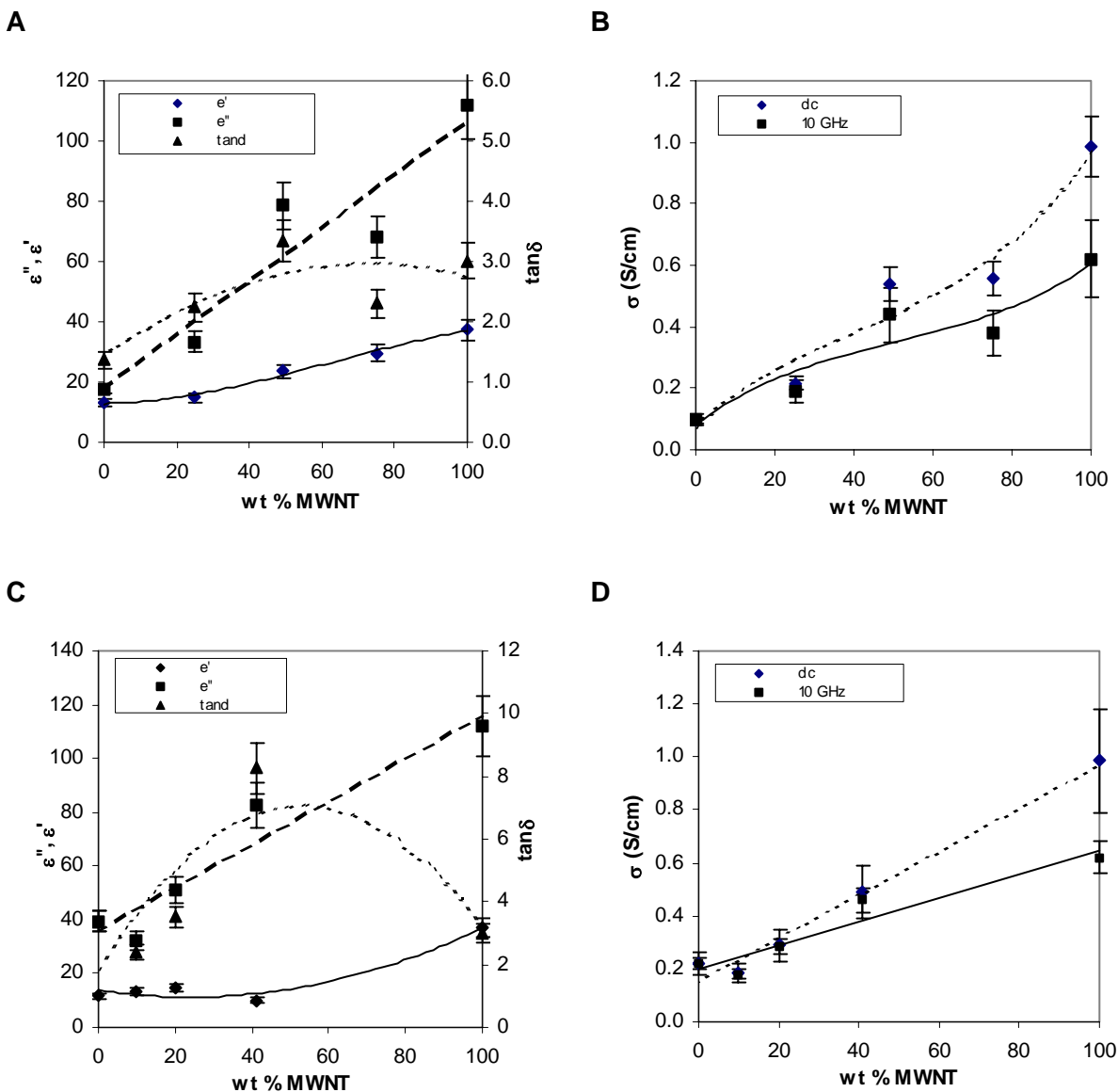


Figure 16. Dielectric properties and conductivities of composite PC3Me (A and B) and PC4Me (C and D). ϵ_r' = real permittivity. ϵ_r'' = complex permittivity. $\tan\delta$ = loss tangent. σ = conductivity.

The magnitude of the increase in $\tan\delta$ compared to composites containing only PANi or MWNT depends on the microwave absorbing properties of the PANi used. When PANi-pTsA1 and MWNT are mixed at the optimum ratio, $\tan\delta$ increases to 3.34, which is over double that of PANi-pTsA1 (1.37) and slightly more than MWNT (3.01). PANi-pTsA2 and MWNT mixed at an optimum ratio gives $\tan\delta$ as high as 8.26, which is 2.5 times PANi-pTsA2 alone and almost 3 times MWNT. Finally, this effect is not limited to PANi-pTsA; PANi-NSA and MWNT at an optimum ratio gave $\tan\delta$ of 4.5, which is nearly 3 times PANi-NSA or 1.5 times the $\tan\delta$ for MWNT (Figure 17). The enhanced absorption at

10 GHz is probably due to the formation of fine conductive paths of MWNTs within the voids of the percolation network of larger PANi particles.

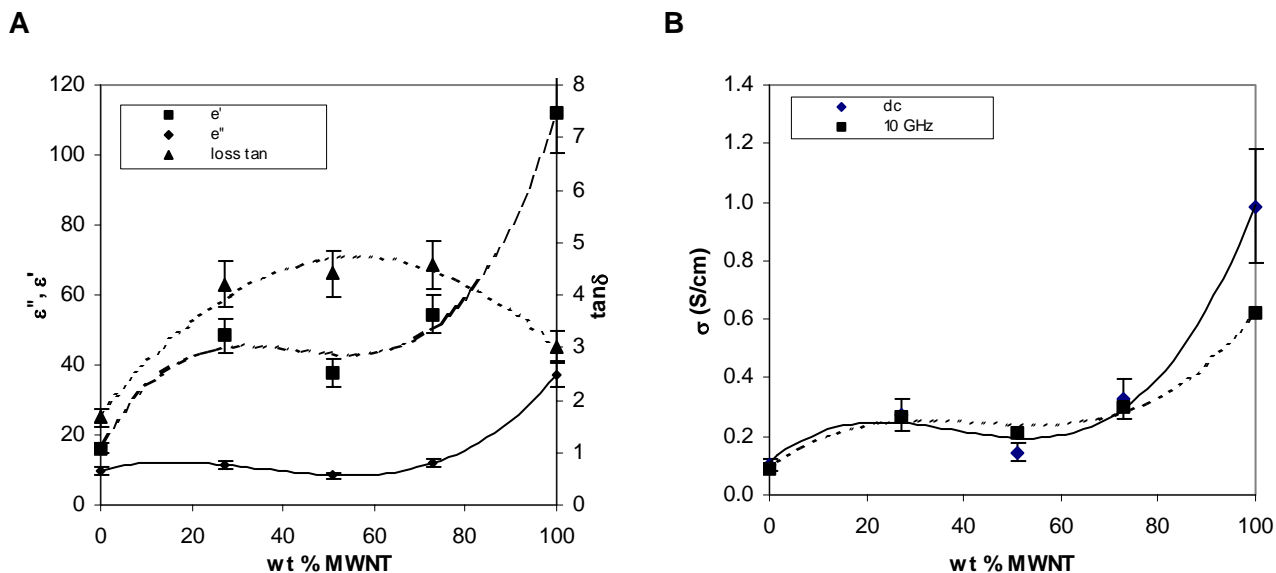


Figure 17. Dielectric properties of composites PC5Me (PANi-NSA mixed with MWNTs *ex situ*) as a function of wt % MWNT. ϵ_r' = real permittivity. ϵ_r'' = complex permittivity. $\tan \delta$ = loss tangent. σ = conductivity.

The enhanced microwave absorption for the composites PC3Me, PC4Me, and PC5Me is unexpected. Near 50 wt % MWNT measured values are significantly different than interpolated values assuming linear mixing. For example, assuming linear mixing for PC5Me (50 wt % MWNT) a $\tan \delta$ of 1.84 is expected, which is lower than the value measured (4.41). Similarly, the predicted $\tan \delta$ values are also lower for PC3Me and PC4Me.

Table 6 lists the measured dielectric parameters for PMMA composites containing PANi, CNTs, and PANi + CNTs (PANi : CNT ~ 1 : 1). For *ex situ* mixed composites containing both PANi and CNTs, theoretical values are also listed, which were calculated from the sum of the values from the two PMMA composites containing PANi and CNTs alone (Table 6). The measured values are all greater than the predicted values by at least a factor of 2. Similar results were obtained when PANi was mixed with MWNTs from another source, Nanocyl SA. SWNTs from Carboxlex did not result in any enhancement of the microwave properties when combined with PANi-NSA. Similar significant enhancements in the microwave absorption by PANi-MWNT/PMMA composites were also observed in preliminary experiments using DBSA, SDS, and NDBSA doped PANi.^v

^v Makeiff, D. A. *Unpublished results.*

Table 6. Dielectric properties of PMMA composites containing PANi, CNT, and PANi + CNT at 10 GHz

Sample	ϵ''	ϵ'	$\tan\delta$
MWNT (Aldrich)	9.31	7.3	1.3
MWNT (Nanocyl SA)	30.7	11.6	2.7
SWNT (Carbolex)	3.5	5.7	0.6
PAni-pTsA1	11.6	8.4	1.4
PCMe3, PAni-pTsA1 + MWNT (Aldrich) ^t	20.9	15.7	1.3
PCMe3, PAni-pTsA1 + MWNT (Aldrich) ^m	78.6	23.5	3.3
PAni-pTsA2	39.4	11.7	3.4
PCMe4, PAni-pTsA2 + MWNT (Aldrich) ^t	48.7	19.0	2.6
PCMe4, PAni-pTsA2 + MWNT (Aldrich) ^m	82.5	10.0	8.3
PAni-NSA	3.71	5.6	0.7
PCMe5, PAni-NSA + MWNT (Aldrich) ^t	13.0	12.9	1.0
PCMe5, PAni-NSA + MWNT (Aldrich) ^m	37.7	8.6	4.4
PAni-NSA + MWNT (Nanocyl SA) ^t	34.4	20.2	1.7
PAni-NSA + MWNT (Nanocyl SA) ^m	54.4	15.7	3.5
PAni-NSA + SWNT (Carbolex) ^t	7.2	11.3	0.6
PAni-NSA + SWNT (Carbolex) ^m	4.7	7.1	0.7

^ttheoretical. ^mmeasured. MWNT = multiwalled (carbon) nanotubes. SWNT = singlewalled (carbon) nanotubes. PANi = polyaniline. pTsA = *para*-toluenesulfonic acid. NSA = 2-naphthalenesulfonic acid. For each composite, the wt % of PANi, MWNT, or SWNT was always ~4.5 %.

Composites containing *ex situ* mixed PANi–pTsA and CNFs (i.e., PC6e in Table 5) did not show improved electrical or microwave absorbing properties (Figure 18). ϵ_r' , ϵ_r'' , and $\tan\delta$ do not change much upon varying the ratio of PANi : CNF. This is not surprising as CNFs in PMMA show relatively poor microwave absorption. Composites PC3Me, PC4Me and PC5Me may be better microwave absorbers because MWNTs and PMMA are more compatible than CNFs and PMMA; CNFs have a higher percolation threshold (Figure15).

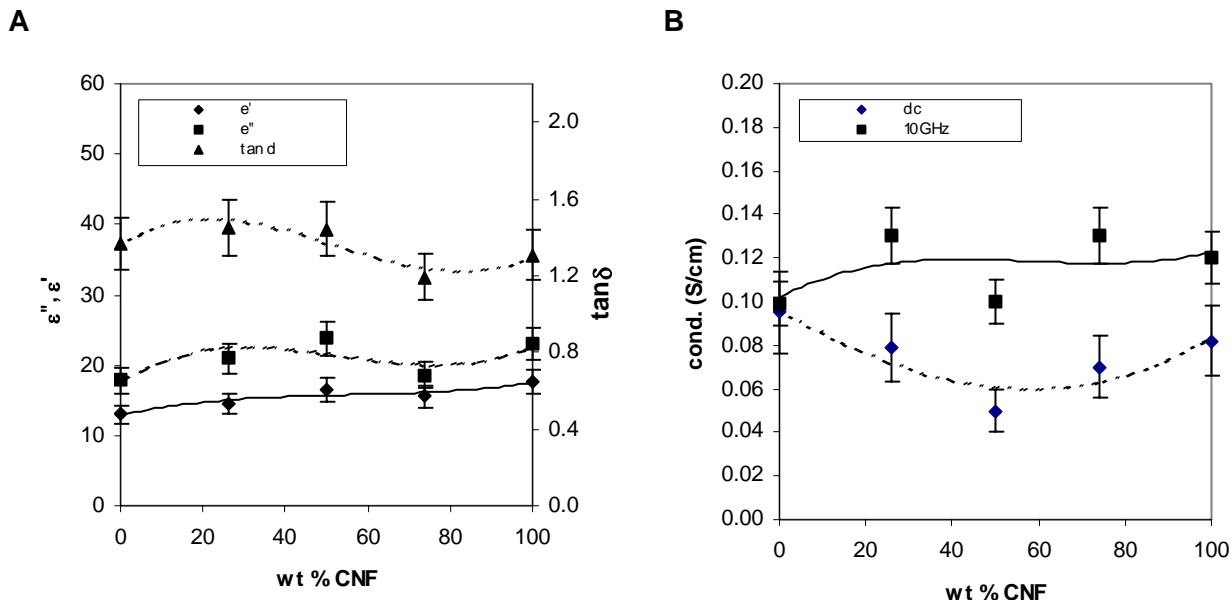


Figure 18. Dielectric properties of PC6e (PAni-pTsA1 mixed with CNF ex situ) as a function of wt % CNF. ϵ_r' = real permittivity. ϵ_r'' = complex permittivity. $\tan \delta$ = loss tangent. σ = conductivity.

3.7 Conclusions

We successfully synthesized PAni–MWNT (and CNF) nanocomposites using a procedure similar to one already reported. This is the first report of PAni–MWNT nanocomposites incorporating pTsA and NSA dopants. Most other reported PAni–CNT nanocomposites involve mineral acid dopants.

SEM and TEM images of the PAni–MWNT (and CNF) nanocomposites showed nano-tubular structures with a rough exterior coated with free PAni particulate. This strongly suggests that PAni prefers to nucleate on the graphite surfaces of CNTs and CNFs rather than in solution. Polymerization is speculated to first occur by the secondary amine functionalization of the carbon nanostructure (CNS) surfaces via reaction with anilinium radical cations or oligomers (Figure 19).^[82] Bonding interactions between the surfaces of MWNTs and CNFs were detected by IR spectroscopy.

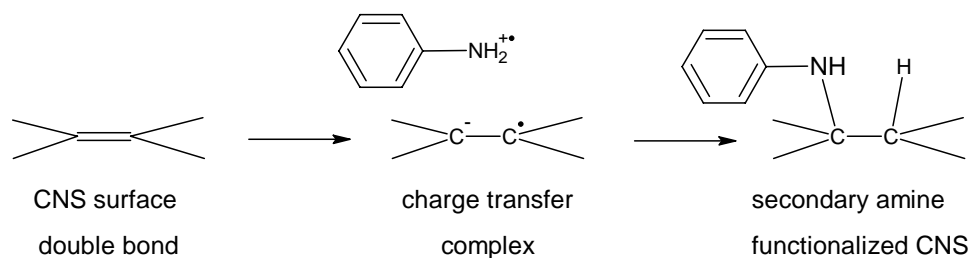


Figure 19. Charge transfer complex formation between aniline and the graphitic carbon nanostructure (CNS) surface, and subsequent secondary amine functionalization.

The PANi–CNS nanocomposite powders synthesized for this report did display higher σ_{dc} than PANi, MWNT, or CNF powders alone. σ_{dc} values reaching 30 and 70 S/cm were observed for PANi–CNF and MWNT, respectively. These values may be further improved upon by optimizing conditions for *in situ* PANi polymerization or by using higher quality MWNTs (or CNFs) that possess fewer structural defects. Polymerization of PANi on MWNTs is feasible for attaining a nanocomposite with higher conductivity at a reduced cost; the mass of inexpensive PANi replaces mass of commercially expensive MWNTs.

PMMA composites containing PANi and MWNTs prepared in this report had good conductivity at low percolation thresholds (i.e., between 0.01 and 1.0 S/cm). PMMA composites containing CNFs or *in situ* PANi–MWNT or PANi–CNF had relatively low conductivity and high percolation thresholds. As a result, CNF/PMMA, *in situ* PANi–MWNT/PMMA, and *in situ* PANi–CNF/PMMA were determined to be poorer microwave absorbers than PANi or MWNTs, despite the higher σ_{dc} of neat PANi–MWNT and PANi–CNF powders. The increase in nanostructure diameter with a PANi coating probably reduces the ability to obtain a fine dispersion. Furthermore, the PANi coated carbon nanostructures are more difficult to fragment into individual nano-sized pieces. Poor matrix compatibility between *in situ* PANi–MWNT/CNF fillers may also be an issue. More detailed microscopy studies may provide confirmation of this.

Finally, improved microwave absorption was found for PMMA composites containing both PANi and MWNTs (i.e., mixed *ex situ*), compared to PANi/PMMA or MWNT/PMMA. At 9 wt % of total conductive filler (PANi and MWNT), the maximum microwave absorption occurs near a ratio of 1 : 1 PANi : MWNT. The microwave properties of these *ex situ* composites can be modulated, either by increasing wt % of total PANi and MWNTs, or by varying the ratio of PANi : MWNT at a fixed total wt %. These enhanced properties may be a result of the mechanism of dispersing of PANi and MWNTs within the PMMA matrix. Dispersion appears to be facilitated by adsorption of MWNTs to larger PANi and PMMA particulates prior to melt processing. We observed adsorption of MWNTs to PANi for this work, while adsorption of MWNTs to PMMA has been reported by others elsewhere.^[109] Maximum microwave absorption may be due to optimal adsorption of MWNTs to the larger PANi and PMMA particles, which is probably when the ratio of PANi : MWNT is 1 : 1.

The preliminary results in this report suggest that PMMA composites containing PANi and MWNTs mixed *ex situ* have potential as microwave absorbers for RAM applications.

Further work is currently underway to optimize conditions for synthesizing PANi-ESs with the highest possible permittivity values in PMMA composites, and to combine them with MWNTs.

4. References

- (1) Pinho, M. S.; Gregori, M. L.; Nunes, R. C. R.; Soares, B. G. *Eur. Polym. J.* **2002**, 38, 2321-2327.
- (2) Annadurai, P.; Mallick, A. K.; Tripathy, D. K. *J. Appl. Poly. Sci.* **2002**, 83, 145-150.
- (3) Joo, J.; Oh, E. J.; Min, G.; MacDiarmid, A. G.; Epstein, A. J. *Synth. Met.* **1995**, 69, 251-254.
- (4) Joo, J.; Oblakowski, Z.; Du, G.; Pouget, J. P.; Oh, E. J.; Wiesinger, J. M.; Min, Y. G.; MacDiarmid, A. G.; Epstein, A. J. *Phys. Rev. B* **1994**, 49, 2977-2980.
- (5) Kaynak, A.; Unsworth, J.; Beard, G. E.; Clout, R. *Mat. Res. Bull.* **1993**, 28, 1109-1125.
- (6) Marchant, S.; Jones, F. R.; Wong, T. P. C.; Wright, P. V. *Synth. Met.* **1998**, 96, 35-41.
- (7) Faez, R.; Martin, I. M.; De Paoli, M.-A.; Rezende, M. C. *Synth. Met.* **2001**, 119, 435 - 436.
- (8) John, H.; Kumar, S. B.; Mathew, K. T.; Joseph, R. *J. Appl. Poly. Sci.* **2002**, 83, 2008-2012.
- (9) Rose, T. L.; D'Antonio, S.; Jillson, M. H.; Kon, A. B.; Suresh, R.; Wang, F. *Synth. Met.* **1997**, 85, 1439-1440.
- (10) Hourquebie, P. B., B.; Dhume, S. *Synth. Met.* **1997**, 85, 1437-1437.
- (11) Olmedo, L.; Hourquebie, P.; Jousse, F. *Adv. Mat.* **1993**, 5, 373-377.
- (12) Epstein, A. J.; Roe, M. G.; Ginder, J. M.; Hajiseyedjavadi, H.; Joo, J. In *U. S. Patent U. S.*, 1996.
- (13) Dhawan, S. K.; Singh, N.; Venkatachalam, S. *Synth. Met* **2002**, 129, 261-267.
- (14) Dhawan, S. K.; Singh, N.; Venkatachalam, S. *Synth. Met* **2002**, 125, 389-393.
- (15) Dhawan, S. K.; Singh, N.; Rodrigues, D. *Science and Technology of Advanced Materials* **2003**, 4, 105-113.
- (16) Colaneri, N. F.; Shacklette, L. W. *IEEE Trans. Instrum. Meas. IM-41* **1992**, 41, 291-297.
- (17) Joo, J.; Lee, C. Y.; Song, H. G.; Kim, J.-W.; Jang, K. S.; Oh, E. J.; Epstein, A. J. *Mol. Cryst. Liq. Cryst.* **1998**, 316, 367-370.
- (18) Joo, J.; Epstein, A. J. *Appl. Phys. Lett.* **1994**, 65, 2278-2280.
- (19) Kohlman, R. S.; Min, Y. G.; MacDiarmid, A. G.; Epstein, A. J. Society of Plastics Engineers Annual Technical Conference (ANTEC), Indianapolis, 1996; p 1412-1416.
- (20) Varma, I. K.; Gupta, G.; Sidhu, C. S. *Macromol. Symp.* **2001**, 164, 401-410.
- (21) Wojkiewicz, J.-L.; Fauveaux, S.; Miane, J.-L. *Synth. Met.* **2003**, 135-136, 127-128.

- (22) Yang, S. C.; Liu, H.; Clark, R. L. In *U. S. Patent Office*; The Board of Governors for Higher Education, State Rhode Island and Providence Plantations: U. S., 2003.
- (23) Watts, P. C. P.; Ponnampalam, D. R.; Hsu, W. K.; Barnes, A.; Chambers, B. *Chem. Phys. Lett.* **2003**, 378, 609-614.
- (24) Grimes, C. A.; Mungle, C.; Kouzoudis, D.; Fang, S.; Eklund, P. C. *Chem. Phys. Lett.* **2000**, 319, 460-464.
- (25) Potschke, P.; Dudkin, S. M.; Alig, I. *Polymer* **2003**, 44, 5023-5030.
- (26) Glatkowski, P., Mack, P., Conroy, J.L., Piche, J.W., Winsor, P.; Eikos, Inc., 2001.
- (27) Knott, E. F.; Shaeffer, J. F.; Tuley, M. T. *Radar Cross Section*; 2nd ed.; Artech House: Norwood, 1993.
- (28) Vinoy, K. J.; Jha, R. M. *Radar Absorbing Materials: from theory to design and characterization*; Kluwer Academic Publishers: Boston, 1996.
- (29) Blythe, A. R. *Electrical Properties of Polymers*; Cambridge University Press: London, 1979.
- (30) Kremer, F.; Schonhals, A. *Broadband Dielectric Spectroscopy*; Springer-Verlag: New York, 2003.
- (31) Chandrasekhar, P. *Conducting Polymers, Fundamentals and Applications: A Practical Approach.*; Kluwer Academic Publishers: London, 1999.
- (32) Pud, A.; Ogurtsov, N.; Korzhenko, A.; Shapoval, G. *Prog. Polym. Sci.* **2003**, 28.
- (33) Battacharya, A.; De, A. *Prog. Solid St. Chem.* **1996**, 24, 141-181.
- (34) Ajayan, P. M. *Chem. Rev.* **1999**, 99, 1787 - 1799.
- (35) Saito, R.; Dresselhaus, G.; Dresselhaus, M. S. *Physical Properties of Carbon Nanotubes*; Imperial College Press: London, 1998.
- (36) Hilding, J., Grulke, E.A., Zhang, Z.G., Lockwood, F. *Journal of Dispersion Science* **2003**, 24, 1-41.
- (37) Mo, Y. H., Kibria, A.K.M.F., Nahm, K.S. *Synth. Met.* **2001**, 122, 443 - 447.
- (38) Mizuki, T., Watanabe, K. Japan, 1989.
- (39) Mickelson, E. T.; Huffman, C. B.; Rinzler, A. G.; Smalley, R. E.; Hauge, R. H.; Margrave, J. L. *Chem. Phys. Lett.* **1998**, 296, 188-194.
- (40) Bahr, J. L.; Yang, J.; Kosynkin, D. V.; Bronikowski, M. J.; Smalley, R. E.; Tour, J. M. *J. Am. Chem. Soc.* **2001**, 123, 6536-6542.
- (41) O'Connell, M.; Boul, P.; Ericson, L. B.; Huffman, C.; Wang, Y.; Haroz, E.; Kuper, C.; Tour, J.; Ausman, K. D.; Smalley, R. E. *Chem. Phys. Lett.* **2001**, 342, 265-271.
- (42) Kang, Y.; Taton, T. A. *J. Am. Chem. Soc.* **2003**, 125, 5650-5651.
- (43) Islam, M. F.; Rojas, E.; Bergey, D. M.; Johnson, A. T.; Yodh, A. G. *Nano Letters* **2003**, 3, 269-273.

- (44) Meincke, O.; Kaempfer, D.; Weikmann, H.; Friedrich, C.; Vathauer, M.; Warth, H. *Polymer* **2004**, *45*, 739-748.
- (45) Smith, J. G. J.; Connell, J. W.; Delozier, D. M.; Lillehei, P. T.; Watson, K. A.; Lin, Y.; Zhou, B.; Sun, Y.-P. *Polymer* **2004**, *45*, 825-836.
- (46) Potschke, P.; Bhattacharyya, A. R.; Janke, A. *Eur. Polym. J.* **2004**, *40*, 137-148.
- (47) Barrau, S.; Demont, P.; Peigney, A.; Laurent, C.; Lacabanne, C. *Macromolecules* **2003**, *36*, 5187-5194.
- (48) Shaffer, M. S. P.; Windle, A.H. *Adv. Mat.* **1999**, *11*, 937-941.
- (49) Sandler, J. K. W.; Kirk, J. E.; Kinloch, I. A.; Shaffer, M. S. P.; Windle, A. H. *Polymer* **2003**, *44*, 5893-5899.
- (50) Valentini, L.; Bavastrello, V.; Stura, E.; Armentano, I.; Nicolini, C.; Kenny, J. M. *Chem. Phys. Lett.* **2004**, *383*, 617-622.
- (51) Zhou, Y.-K.; He, B.-L.; Zhou, W.-J.; Huang, J.; Li, X.-H.; Wu, B.; Li, H.-L. *Electrochimica Acta* **2004**, *49*, 257-262.
- (52) Ramamurthy, P. C.; Harrell, W. R.; Gregory, R. V.; Sadanadan, B.; Rao, A. M. *Synth. Met.* **2003**, *137*, 1497-1498.
- (53) Feng, W.; Bai, X. D.; Lian, Y. Q.; Liang, J.; Wang, X. G.; Yoshino, K. *Carbon* **2003**, *41*, 1551-1557.
- (54) Wei, Z. W., M.; Lin, T.; Dai, L. *Adv. Mater.* **2003**, *15*, 136-139.
- (55) Huang, J.-E.; Li, X.-H.; Xu, J.-C.; Li, H.-L. *Carbon* **2003**, *41*, 2731-2736.
- (56) Tchmutin, I. A.; Ponomarenko, A. T.; Krinichnaya, E. P.; Kozub, G. I.; Efimov, O. N. *Carbon* **2003**, *41*, 1391-1395.
- (57) Maser, W. K.; Benito, A. M.; Callejas, M. A.; Seeger, T.; Martinez, M. T.; Schreiber, J.; Muszynski, J.; Chauvet, O.; Osvath, Z.; Koos, A. A.; Biro, L. P. *Mat. Sci. & Eng. C* **2003**, *23*, 87-91.
- (58) Baibarac, M.; Baltog, I.; Lefrant, S.; Mevellec, J. Y.; Chauvet, O. *Chem. Mater.* **2003**, *15*, 4149-4156.
- (59) Zengin, H.; Zhou, W.; Jin, J.; Czerw, R.; Smith, J. D. W.; Echegoyen, L.; Carroll, D. L.; Foulger, S. H.; Ballato, J. *Adv. Mat.* **2002**, *14*, 1480-1483.
- (60) Valter, B.; Ram, M. K.; Nicolini, C. *Langmuir* **2002**, *18*, 1535-1541.
- (61) Deng, J.; Ding, X.; Zhang, W.; Peng, Y.; Wang, J.; Long, X.; Li, P.; Chan, A. S. C. *Eur. Polym. J.* **2002**, *38*, 2497-2501.
- (62) Gao, M.; Huang, S.; Dai, L.; Wallace, G.; Gao, R.; Wang, Z. *Angew. Chem. Int. Ed.* **2000**, *39*, 3664-3667.
- (63) Iroh, J. O.; Rjagopalan, R. *J. App. Polym. Sci.* **2000**, *76*, 1503-1509.
- (64) Cochet, M.; Maser, W. K.; Benito, A. M.; Callejas, M. A.; Martinez, M. T.; Benoit, J. M.; Schreiber, J.; Chauvet, O. *Chem. Commun.* **2001**, 1450-1451.

- (65) Hassanien, A.; Gao, M.; Tokumoto, M.; Dai, L. *Chem. Phys. Lett.* **2001**, *342*, 479-484.
- (66) Downs, C.; Nugent, J.; Ajayan, P. M.; Duquette, D. J.; Santhanam, S. V. *Adv. Mater.* **1999**, *11*, 1028-1031.
- (67) Xiao, Q.; Zhou, X. *Electrochim. Acta* **2003**, *48*, 575-580.
- (68) Chen, J. H.; Huang, Z. P.; Wang, D. Z.; Yang, S. X.; Li, W. Z.; Wen, J. G.; Ren, Z. F. *Synth. Met* **2002**, *125*, 289-294.
- (69) Hughes, M.; Shaffer, M. S. P.; Renouf, A. C.; Singh, C.; Chen, G. Z.; Fray, D. J.; Windle, A. H. *Adv. Mat.* **2002**, *14*, 382-385.
- (70) Chen, G. Z.; Shaffer, M. S. P.; Coleby, D.; Dixon, G.; Zhou, W.; Fray, J. D.; Windle, A. H. *Adv. Mater.* **2000**, *12*, 522-526.
- (71) Fan, J.; Wan, M.; Zhu, D.; Chang, B.; Pan, Z.; Xie, S. *Synth. Met.* **1999**, *102*, 1266-1267.
- (72) Musa, I.; Baxendale, M.; Amaratunga, G. A. J.; Eccleston, W. *Synth. Met.* **1999**, *102*, 1250.
- (73) Woo, H. S.; Czerw, R.; Webster, S.; Carroll, D. L.; Park, J. W.; Lee, J. H. *Synth. Met.* **2001**, *116*, 369-372.
- (74) Dalton, A. B.; Stephan, C.; Coleman, J. N.; McCarthy, B.; Ajayan, P. M.; Lefrant, S.; Bernier, P.; Blau, W. J.; Byrne, H. J. *J. Phys. Chem. B* **2000**, *104*, 10012-10016.
- (75) Ago, H.; Petritsch, K.; Shaffer, M. S. P.; Windle, A. H.; Friend, R. H. *Adv. Mater.* **1999**, *11*, 1281-1285.
- (76) McCarthy, B., Dalton, A.B., Coleman, J.N., Byrne, H.J., Bernier, P., Blau, W.J. *Chem. Phys. Lett.* **2001**, *350*, 27-32.
- (77) Steuerman, D. W.; Star, A.; Narizzano, R.; Choi, H.; Ries, R. S.; Nicolini, C.; Stoddart, J. F.; Heath, J. R. *J. Phys. Chem. B* **2002**, *106*, 3124-3130.
- (78) Curran, S. A.; Ajayan, P. M.; Blau, W. J.; Carroll, D. L.; Coleman, J. N.; Dalton, A. B.; Davey, A. P.; Drury, A.; McCarthy, B.; Maier, S.; Strevens, A. *Adv. Mater.* **1998**, *10*, 1091-1093.
- (79) Woo, H. S.; Czerw, R.; Webster, S.; Carroll, D. L.; Ballato, J.; Strevens, A. E.; O'Brien, D.; Blau, W. J. *Appl. Phys. Lett.* **2000**, *77*, 1393-1395.
- (80) Panhuis, M. i. h.; Maiti, A.; Dalton, A. B.; van den Noort, A.; Coleman, J. N.; McCarthy, B.; Blau, W. J. *J. Phys. Chem. B.* **2003**, *107*, 478-482.
- (81) Cochet, M., Maser, W.K., Benito, A.M., Callejas, M.A., Martinez, M.T., Benoit, J.M., Schreiber, J., Chauvet, O. *Chem. Commun.* **2001**, 1450-1451.
- (82) Sun, Y.; Wilson, S. R.; Schuster, D. I. *J. Am. Chem. Soc.* **2001**, *123*, 5348 - 5349.
- (83) Taipalus, R.; Harmia, T.; Friedrich, K. *Polymer Composites* **2000**, *21*, 396-416.
- (84) Cao, Y.; Andreatta, A.; Heeger, A. J.; Smith, P. *Polymer* **1989**, *30*, 2305-2311.

- (85) Williams, T. C.; Stuchly, M. A.; Saville, P. *IEEE Trans. Microwave Theory Tech.* **2003**, *51*, 1560-1566.
- (86) Baibarac, M.; Baltog, I.; Lefrant, S.; Mevellec, J. Y.; Chauvet, O. *Chem. Mater.* **2003**, *ASAP*.
- (87) Wan, M.; Li, J.; Li, S. *Polymers for Advanced Technologies* **2001**, *12*, 651-657.
- (88) MacDiarmid, A. G.; Epstein, A. J. *Faraday Discussions* **1989**, *88*, 317 - 332.
- (89) Genies, E. M.; Boyle, A.; Lapkowski, M.; Tsintavis, C. *Synth. Met.* **1990**, 139 - 182.
- (90) Coleman, J. N., Curran, S., Dalton, A.B., Davey, A.P., McCarthy, B., Blau, W., Barklie, R.C. *Synth. Met.* **1999**, *102*, 1174-1175.
- (91) Dahman, S. J. In *Handbook of Polymer Blends and Composites*; Vasile, C., Ed.; Rapra Technology Ltd.: Shawbury, Shrewsbury, Shropshire, 2002; Vol. 2.
- (92) Morgan, H.; Foot, P. J. S.; Brooks, N. W. *J. Mater. Sci.* **2001**, *36*, 5369-5377.
- (93) Cho, M. S.; Cho, Y. H.; Choi, H. J.; Jhon, M. S. *Synth. Met.* **2003**, *135-136*, 15-16.
- (94) Pereira da Silva, J. E.; Cordoba de Torresi, S. I.; Temperini, M. L. A. *Synth. Met* **2001**, *119*, 331-332.
- (95) Pereira da Silva, J. E.; Temperini, M. L. A.; Cordoba de Torresi, S. I. *Synth. Met.* **2003**, *135-136*, 134.
- (96) Zhang, Q. H.; Gao, J.; Wang, X. H.; Chen, D. J.; Jing, X. B. *Synth. Met.* **2003**, *135-136*, 479-480.
- (97) Juvin, P.; Hasik, M.; Fraysse, J.; Planes, J.; Pron, A.; Kulsezewicz-Bajer, I. *J. App. Polym. Sci.* **1999**, *74*, 471-479.
- (98) Dutta, P.; De, S. K.; Chatterjee, S. *Plastics, Rubber and Composites* **2002**, *31*, 158-161.
- (99) Subramaniam, C. K.; Kaiser, A. B.; Gilberd, P. W.; Liu, C.-J. *Solid State Commun.* **1996**, *97*, 235-238.
- (100) Wan, M.; Li, M.; Li, J.; Liu, Z. *Thin Solid Films* **1995**, *259*, 188-193.
- (101) Kaiser, A. B.; Liu, C.-J.; Gilberd, P. W.; Chapman, B.; Kemp, N. T.; Wessling, B.; Partridge, A. C.; Smith, W. T.; Shapiro, J. S. *Synth. Met.* **1997**, *84*, 699-702.
- (102) Niziol, J.; Laska, J. *Synth. Met.* **1999**, *101*, 720-721.
- (103) Cadenas, J. L.; Hu, H. *Solar Energy Materials and Solar Cells* **1998**, *55*, 105-112.
- (104) Lamy de la Chapelle, M.; Stephan, C.; Nguyen, T. P.; Lefrant, S.; Journet, C.; Bernier, P.; Munoz, E.; Benito, A.; Maser, W. K.; Martinez, M. T.; de la Fuente, G. F.; Guillard, T.; Flamant, G.; Alvarez, L.; Laplaze, D. *Synth. Met.* **1999**, *103*, 2510-2512.
- (105) Choi, H. J.; Cho, Y. H.; Cho, M. S. *Int. J. Mod. Phy. B* **2002**, *16*, 2507-2513.
- (106) Stephan, C.; Nguyen, T. P.; Lamy de la Chapelle, M.; Lefrant, S.; Journet, C.; Bernier, P. *Synth. Met.* **2000**, *108*, 139-149.

- (107) Jia, Z.; Wang, Z.; Xu, C.; Liang, J.; Wei, B.; Wu, D.; Zhu, S. *Mater. Sci. Eng. A* **1999**, *271*, 395-400.
- (108) Philip, B.; Abraham, J.; Chandrasekhar, A.; Varadan, V. K. *Smart Mater. Struct.* **2003**, *12*, 935-939.
- (109) Cooper, C. A.; Ravich, D.; Lips, D.; Mayer, J.; Wagner, H. D. *Comp. Sci. Tech.* **2002**, *62*, 1105-1112.

List of symbols/abbreviations/acronyms/initialisms

APS	ammonium persulfate
BSA	benzenesulfonic acid
CNT	carbon nanotube (general)
CNF	carbon nanofibre
CNS	carbon nanostructure
CSA	camphor sulfonic acid
DBSA	dodecylbenzenesulfonic acid
DND	Department of National Defence
EB	emeraldine base
ϵ^*	complex permittivity
ϵ'	real permittivity
ϵ''	imaginary permittivity
ES	emeraldine salt
ex situ	Latin meaning out of the natural or original position or place (i.e. outside/after a reaction)
FT-IR	Fourier Transform Infrared (Spectroscopy)
h	hours
in situ	Latin meaning “in the natural or original position or place” (i.e. directly in/during a reaction)
GHz	Giga Hertz
LB	leucoemeraldine base
min	minutes
MWNT	multiwalled (carbon) nanotube

NT	nanotube
NSA	2-naphthalene sulfonic acid
NDBSA	1,5-naphthalenedisulfonic acid
N1i	polyaniline- <i>para</i> -toluenesulfonate coated multiwalled (carbon) nanotube nanocomposites
N2i	polyaniline- <i>para</i> -toluene sulfonate coated carbon nanofibre nanocomposites
N3i	polyaniline-2-naphthalenesulfonate coated carbon nanofibre nanocomposites
N1e	polyaniline- <i>para</i> -toluenesulfonate mixed with multiwalled (carbon) nanotubes
N2e	polyaniline- <i>para</i> -toluenesulfonate mixed with carbon nanofibres
σ_{dc}	DC conductivity
σ_{mw}	microwave conductivity (10 GHz)
σ_{ac}	AC conductivity
PAni	polyaniline
PB	pernigraniline base
p_c	percolation threshold
PMMA	poly(methyl methacrylate)
pTsA	<i>para</i> -toluenesulfonic acid
SEM	scanning electron microscopy
SWNT	singlewalled (carbon) nanotube
$\tan\delta$	loss tangent
TEM	transmission electron microscopy
vide infra	Latin meaning “see below”
vide supra	Latin meaning “see above”

Distribution list

Note No.: DRDC ATLANTIC DLP/

LIST PART 1: CONTROLLED BY DRDC ATLANTIC LIBRARY

<u>2</u>	DRDC ATLANTIC LIBRARY FILE COPIES
<u>4</u>	DRDC ATLANTIC LIBRARY (SPARES)
<u>1</u>	DLP LIBRARY
<u>3</u>	AUTHORS

<u>10</u>	TOTAL LIST PART 1
-----------	-------------------

LIST PART 2: DISTRIBUTED BY DRDKIM 3

<u>1</u>	NDHQ/ DRDKIM 3 (scanned and stored as black & white image, low resolution - laser reprints available on request)
<u>1</u>	NDHQ/DMSS
<u>1</u>	NDHQ/DMSS 2-5-4
<u>1</u>	NDHQ/DMPPD 4
<u>1</u>	NDHQ/DMRS 7
<u>1</u>	NDHQ/MRCC

<u>6</u>	TOTAL LIST PART 2
----------	-------------------

16 TOTAL COPIES REQUIRED

Original document held by DRDC ATLANTIC Drafting Office

Any requests by DRDC ATLANTIC staff for extra copies of this document should be directed to the DRDC ATLANTIC LIBRARY.

DOCUMENT CONTROL DATA SHEET

1a. PERFORMING AGENCY DRDC Atlantic		2. SECURITY CLASSIFICATION UNCLASSIFIED –
1b. PUBLISHING AGENCY DRDC Atlantic		
3. TITLE (U) Complex Permittivity of Polyaniline/Carbon Nanotube and Nanofibre Nanocomposites in the X–band: PMMA Composites / Complex Permittivity of Polyaniline/Carbon Nanotube and Nanofibre Nanocomposites in the X–band: PMMA Composites		
4. AUTHORS Darren Makeiff Trish Huber Paul Saville		
5. DATE OF PUBLICATION May 16 , 2005		6. NO. OF PAGES 50
7. DESCRIPTIVE NOTES		
8. SPONSORING/MONITORING/CONTRACTING/TASKING AGENCY Sponsoring Agency: Monitoring Agency: Contracting Agency : Tasking Agency:		
9. ORIGINATORS DOCUMENT NO. Technical Memorandum TM 2004–124	10. CONTRACT GRANT AND/OR PROJECT NO. 11gm18	11. OTHER DOCUMENT NOS.
12. DOCUMENT RELEASABILITY Unlimited distribution		
13. DOCUMENT ANNOUNCEMENT Unlimited announcement		

14. ABSTRACT

(U) Polymer composites incorporating polyaniline (PAni) and multiwalled carbon nanotubes (MWNTs) as conductive filler were synthesized and characterized using FT-IR spectroscopy, SEM, TEM, and dc conductivity measurements. The pure nanocomposite powders were significantly more conductive than PAni, MWNT, or CNFs alone. PAni, MWNT, CNFs, PAni-coated MWNT (PAni-MWNT), and PAni-coated CNF (PAni-CNF) nanocomposites were also incorporated as conductive filler into the insulating matrix, PMMA, to produce a rigid and conductive composite material with well-defined shape. The microwave properties of these composites were examined by determining the complex permittivity from transmission-reflection waveguide measurements in the X-band (8–12 GHz). PMMA composites containing PAni-MWNT or PAni-CNFs poorer, while PMMA composites containing PAni and MWNT mixed ex situ were better microwave absorbers than composites containing only PAni or MWNTs.

(U) Des composites polymères contenant de la polyaniline (PAni) et des nanotubes de carbone multiparois (NTMP) servant d'agents conducteurs ont été synthétisés et caractérisés par spectroscopie FTIR, MEB, MET et en mesurant la conductivité en courant continu. Les poudres de nanocomposites purs étaient substantiellement plus conductrices que la polyaniline, les NTMP ou les nanofibres de carbone (NFC) seuls. Des nanocomposites de polyaniline, de NTMP, de NFC, de NTMP recouverts de polyaniline (PAni-NTMP) et de NFC recouvertes de polyaniline (PAni-NFC) ont également été incorporés comme agents conducteurs dans la matrice isolante de PMMA pour produire un matériau composite rigide et conducteur ayant une forme bien définie. Les propriétés hyperfréquence de ces composites ont été examinées en déterminant la permittivité complexe à partir de mesures de transmission et de réflexion à l'aide d'un guide d'ondes dans la bande X (8–12 GHz). Les composites de PMMA contenant des PAni-NTMP ou des PAni-NFC se sont révélés être de moins bons absorbeurs de micro-ondes que les composites contenant de la polyaniline ou des NTMP seulement, alors que les composites de PMMA contenant de la polyaniline et des NTMP mélangés ex situ se sont révélés être de meilleurs absorbeurs de micro-ondes.

15. KEYWORDS, DESCRIPTORS or IDENTIFIERS

(U) Polyaniline, Permittivity, Carbon Nanotube, Carbon Nanofibre, Nanocomposite, Multiwalled nanotubes, X-band, polymethylmethacrylate, PMMA

This page intentionally left blank.

Defence R&D Canada

Canada's leader in defence
and National Security
Science and Technology

R & D pour la défense Canada

Chef de file au Canada en matière
de science et de technologie pour
la défense et la sécurité nationale



www.drdc-rddc.gc.ca